Science and Technology Indonesia
e-ISSN:2580-4391 *p*-ISSN:2580-4405
Vol. 11, No. 4, October 2026

Research Paper

Structural Characterization and Immunogenic Evaluation of a 50 kDa Thyroid Peroxidase Fraction Isolated from Hypothyroid Patient Serum

Devi Ramadani[1], Aulanni'am Aulanni'am[1*], Muh. Fikry Baharuddin[1], Almas Dwi Khairana[1], Saidun Fiddaroini[1], Muhammad Fikri Nur[1], Hilman Nurmahdi[1], Wibi Riawan[2], Arie Srihardyastutie[1], Akhmad Sabarudin[1], Dyah Kinasih Wuragil[3], Rulli Rosandi[4], Achmad Rudijanto[5], Ahmad Lubab[6]

[1]*Department of Chemistry, Faculty of Mathematics and Natural Science, Brawijaya University, Malang, East Java, 65145, Indonesia*
[2]*Faculty of Medicine, Brawijaya University, Malang, East Java, 65145, Indonesia*
[3]*Faculty of Veterinary Medicine, Brawijaya University, Malang, East Java, 65145, Indonesia*
[4]*Metabolic and Endocrinology Division, Department of Internal Medicine of Saiful Anwar Hospital, Brawijaya University, Malang, East Java, 65145, Indonesia*
[5]*Endocrinology Divison, Department of Pediatrics of Saiful Anwar General Hospital, Brawijaya University, Malang, East Java, 65145, Indonesia*
[6]*Department of Mathematics, Faculty of Science And Technology, Sunan Ampel State Islamic University, Surabaya, East Java, 65145, Indonesia*
*__Corresponding author__: aulani@ub.ac.id

Abstract
Thyroid peroxidase (TPO) is a key enzyme involved in thyroid hormone biosynthesis and one of the major autoantigens in autoimmune thyroid disease. However, studies investigating immunoreactive serum-derived TPO-related protein fractions remain limited. This study aimed to isolate an approximately 50 kDa immunoreactive protein fraction from the serum of hypothyroid patients, characterize its biochemical properties, and evaluate its immunogenicity for rabbit polyclonal antibody production. Serum samples were initially characterized based on anti-TPO antibody levels and total protein concentration. Rabbits were immunized with the isolated protein, and the resulting immune response was evaluated by indirect ELISA, SDS-PAGE, Western blotting, histopathology, and immunohistochemistry. SDS-PAGE consistently revealed a distinct protein band at approximately 50 kDa. ATR-FTIR analysis demonstrated characteristic protein-associated functional groups, while LC-MS/MS confirmed the proteinaceous nature of the isolated fraction through amino acid composition analysis. Immunization induced a progressive increase in anti-TPO IgG levels, and the purified rabbit IgG exhibited the expected electrophoretic profile under reducing and non-reducing conditions. Western blot analysis demonstrated that the generated polyclonal antibodies recognized the isolated approximately 50 kDa protein fraction, whereas no signal was detected in the secondary antibody-only control. Histopathological and immunohistochemical analyses further supported activation of the immune response following immunization. These findings demonstrate that the isolated approximately 50 kDa immunoreactive protein fraction possesses biochemical and immunogenic properties and has potential as an experimental immunogen for polyclonal antibody production.

Keywords
Hypothyroidism, TPO, Autoimmune, CD4$^+$ T Expression, Immunohistochemistry

Received: 12 May 2026, Accepted: 6 August 2026
https://doi.org/10.26554/sti.2026.11.4.1476-1496

1. INTRODUCTION

Hypothyroidism is one of the most prevalent endocrine disorders worldwide and remains a major public health concern due to its high incidence, chronic progression, and significant impact on metabolic, cardiovascular, reproductive, and neurocognitive. The condition is characterized by insufficient production of thyroid hormones, particularly thyroxine (T4) and triiodothyronine (T3), resulting in systemic metabolic dysregulation functions. Current epidemiological data indicate that hypothyroidism affects millions of individuals globally, with a substantially higher prevalence in women and older populations. In developing countries, including many regions of Asia and Africa, iodine deficiency remains the principal cause of hypothyroidism, particularly in areas where nutritional iodine intake is inadequate (Calsolaro et al., 2019; Pushpagiri et al., 2015; Trifanescu and Poiana, 2019; Yadav et al., 2021). However, in iodine-sufficient regions, autoimmune thyroid disease (AITD), especially Hashimoto's thyroiditis, has emerged as the dominant cause of primary hypothyroidism. The increasing global incidence of autoimmune hypothyroidism has drawn significant clinical attention because the disease often progresses silently from subclinical thyroid dysfunction to irreversible

glandular damage before clinical diagnosis is established (Patagar and Rudrappa, 2022).

Hashimoto's thyroiditis represents the most common autoimmune cause of hypothyroidism and is characterized by chronic lymphocytic infiltration of the thyroid gland, progressive follicular destruction, and sustained production of thyroid autoantibodies. Among these, anti-thyroid peroxidase antibodies (anti-TPO) are the most clinically relevant biomarkers and are detected in approximately 90–95% of patients with Hashimoto's thyroiditis (Hu et al., 2022; Klubo-Gwiezdzinska and Wartofsky, 2022; Ragusa et al., 2019). Elevated anti-TPO levels are strongly associated with subclinical hypothyroidism, progression to overt hypothyroidism, and increased risk of concurrent autoimmune disorders such as type 1 diabetes mellitus, rheumatoid arthritis, systemic lupus erythematosus, and celiac disease (Antonelli et al., 2015; Siriwardhane et al., 2019). Several recent clinical reports have shown that a large proportion of patients with elevated thyroid-stimulating hormone (TSH) but normal circulating T3 and T4 levels already exhibit significantly increased anti-TPO titers, indicating that autoimmune destruction begins long before hormonal failure becomes clinically apparent. This creates a major diagnostic challenge, particularly in early disease screening, because conventional thyroid function tests alone are often insufficient to detect early injury (Ferrari et al., 2021; Siriwardhane et al., 2019).

Thyroid peroxidase (TPO) is the key enzyme responsible for thyroid hormone biosynthesis and serves as the principal autoantigen in autoimmune thyroid disease. TPO is a glycosylated, membrane-bound heme-containing peroxidase localized on the apical membrane of thyroid follicular cells. It catalyzes iodide oxidation, iodination of tyrosyl residues on thyroglobulin, and coupling reactions necessary for the formation of T3 and T4 (Benvenga and Vita, 2018; Godlewska et al., 2017, 2019). Structurally, TPO consists of a large extracellular domain, a single transmembrane region, and a short intracellular tail. The extracellular domain contains several highly conserved functional regions, including a peroxidase-like catalytic domain, complement control protein (CCP)-like domain, and epidermal growth factor (EGF)-like domain. Recent structural biology studies have demonstrated that these domains form a highly stable three-dimensional conformation maintained by extensive disulfide bonding, which is essential for enzymatic activity and immune recognition. Importantly, anti-TPO antibodies predominantly recognize conformational epitopes rather than linear peptide sequences, with the major immunodominant regions (IDR-A and IDR-B) located mainly within the peroxidase-like domain. These antibody-binding sites are spatially distinct from the catalytic center, suggesting that anti-TPO positivity reflects immune recognition of structural epitopes rather than direct catalytic inhibition (Le et al., 2015; Ma et al., 2015; Williams et al., 2020).

Current state-of-the-art studies in autoimmune hypothyroidism have largely focused on serological detection of anti-TPO using ELISA, chemiluminescent immunoassays, and electrochemiluminescence platforms. While these methods are highly sensitive for clinical diagnosis, they provide limited information regarding the structural characteristics, molecular heterogeneity, and immunogenic properties of native TPO derived from hypothyroid patients (Ali et al., 2025; Jin et al., 2025; Shawkat Kawther et al., 2022). Recombinant TPO fragments have been widely used for epitope mapping and immunological studies; however, these systems often fail to preserve native glycosylation patterns and conformational epitopes required for authentic antibody recognition. Furthermore, most available studies emphasize antibody quantification rather than direct biochemical characterization of patient-derived TPO protein. This creates a significant gap in understanding how structural variation of native TPO influences immune recognition and downstream autoimmune responses (Aulanni'am et al., 2018; Le et al., 2015; Williams et al., 2020).

Previous methodological approaches for TPO characterization have included SDS-PAGE for molecular weight estimation, Western blotting for immunoreactivity confirmation, and limited LC-MS-based peptide identification. Some studies have employed FTIR to evaluate protein secondary structure and glycosylation-associated spectral signatures, while others used mass spectrometry to identify peptide fragments and confirm protein identity. However, these approaches are often performed separately, resulting in fragmented molecular information rather than an integrated characterization platform (Neto et al., 2022; Ramadani et al., 2024; Tater et al., 2021). In addition, previous immunogenicity studies commonly relied on commercially available purified antigens or recombinant proteins for animal immunization, which may not accurately reflect the immunological behavior of naturally occurring patient-derived TPO. This limitation is particularly important because autoimmune recognition in Hashimoto's thyroiditis depends strongly on conformational antigenic determinants preserved only in native protein structures (Aulanni'am et al., 2018, 2024; Ramadani et al., 2024).

The present study offers a significant methodological advantage by integrating comprehensive biochemical characterization of native TPO isolated directly from sera of hypothyroid patients with in vivo immunogenicity evaluation using a polyclonal antibody production model (Aulanni'am, 2023; Ramadani et al., 2024). TPO was isolated and characterized using sequential SDS-PAGE with silver staining, Fourier transform infrared spectroscopy (FTIR), and liquid chromatography-mass spectrometry (LC-MS), allowing simultaneous evaluation of molecular weight distribution, structural functional groups, protein integrity, and peptide-level identity confirmation. Silver staining provides superior sensitivity for detecting low-abundance serum proteins, while FTIR enables structural fingerprinting of protein functional groups and glycosylation-associated signals. LC-MS provides high-resolution peptide validation and molecular confirmation of isolated TPO. This integrated analytical strategy offers a more accurate representation of native TPO architecture compared with recombinant antigen systems (Huang et al., 2018; Liu et al., 2016; Villela et al., 2018).

Moreover, this study extends beyond molecular characterization by evaluating the biological immunogenicity of isolated TPO through polyclonal antibody induction in New Zealand White rabbits. Unlike conventional studies restricted to in vitro serological assays, this approach enables direct assessment of adaptive immune activation in vivo. Since autoimmune hypothyroidism is fundamentally mediated by dysregulated $CD4^+$ T-cell–dependent humoral immunity, the investigation of splenic CD4 cell expression provides critical insight into antigen-driven immune activation. The spleen serves as a major secondary lymphoid organ where antigen presentation, T-cell activation, and B-cell differentiation occur, making it a highly relevant target for immunological assessment (Teijaro et al., 2011; Zhu et al., 2010). In parallel, thymic TPO expression analysis offers important information regarding central immune tolerance and the potential breakdown of self-tolerance mechanisms contributing to autoimmune disease. Immunohistochemistry supported by histopathological analysis of both spleen and thymus therefore provides a mechanistic bridge between molecular antigen characterization and systemic immune response (Marx et al., 2021; Takaba and Takayanagi, 2017).

Based on these considerations, the present study aimed to isolate an immunoreactive approximately 50 kDa protein fraction from the serum of hypothyroid patients and to characterize its biochemical and immunological properties using complementary analytical approaches, including SDS-PAGE, ATR-FTIR, amino acid composition analysis, and Western blotting. Furthermore, the isolated protein fraction was evaluated as an immunogen for the production of rabbit polyclonal antibodies, and the resulting immune response was assessed by ELISA and immunoblotting. This study provides a preliminary evaluation of the isolated protein fraction as an experimental immunogen.

2. EXPERIMENTAL SECTION

2.1 Materials and Reagent

Human serum samples were obtained from clinically diagnosed hypothyroid patients with elevated anti-thyroid peroxidase antibody (anti-TPO) levels through collaboration with the Endocrinology Division, Saiful Anwar General Hospital, Malang, Indonesia. New Zealand White rabbits (Oryctolagus cuniculus), male, aged 3 - 4 months and weighing 2.0 – 2.5 kg, were used for polyclonal antibody production and immunogenicity evaluation.

The chemicals used for thyroid peroxidase (TPO) isolation included phosphate-buffered saline with Tween-20 (PBST), phenylmethylsulfonyl fluoride (PMSF), absolute ethanol, cold ethanol (Merck, Darmstadt, Germany), and Tris-HCl buffer (Sigma-Aldrich, St. Louis, MO, USA). Protein concentration measurements were performed using NanoDrop^{TM} spectro photometry compatible reagents and biuret reagents. For protein separation and characterization, sodium dodecyl sulfate-polyacrylamide gel electrophoresis (SDS-PAGE) reagents included 30% acrylamide/ bis-acrylamide solution, sodium dodecyl sulfate (SDS), ammonium persulfate (APS), N,N,N′,N′-tetramethylethylene diamine (TEMED), Tris-HCl, glycerol, bromophenol blue, β-mercaptoethanol, and Spectra^{TM} Multi Color High Range Protein Ladder (ThermoFisher). Nitrocellulose membranes for Western blot analysis were purchased from Bio-Rad Laboratories (USA).

Silver staining reagents consisted of ethanol (Merck, Germany), glacial acetic acid (Merck, Germany), sodium thiosulfate pentahydrate ($Na_2S_2O_3{\cdot}5H_2O$; Sigma-Aldrich, USA), silver nitrate ($AgNO_3$; Merck, Germany), sodium carbonate (Na_2CO_3; Merck, Germany), paraformaldehyde, and acetic acid (Merck, Germany).Fourier transform infrared spectroscopy (FTIR) analysis used analytical-grade liquid samples without additional derivatization and was performed using ATR-compatible preparations. Amino acid analysis by LC-MS/MS employed 6 N hydrochloric acid (HCl; Merck, Germany), 4 N sodium hydroxide (NaOH; Merck, Germany), 0.1 N HCl, formic acid (LC-MS grade; Merck, Germany), acetonitrile (LC-MS grade; Merck, Germany), ammonium formate (Sigma-Aldrich, USA), and amino acid standard solutions (Shimadzu, Kyoto, Japan).

For rabbit immunization, Complete Freund's Adjuvant (CFA) and Incomplete Freund's Adjuvant (IFA) were obtained from Sigma-Aldrich (St. Louis, MO, USA). Blood collection was performed using sterile syringes and 24G needles (OneMed, Indonesia) and Vaculab® vacutainer tubes. Immunoglobulin G (IgG) isolation used 50% saturated ammonium sulfate (SAS; Merck, CAS No. 7783-20-2), phosphate buffer (0.1–0.2 M), dialysis solution, and Tris-HCl buffer(Sigma - Aldrich, USA). CBB staining reagents consisted of Coomassie Brilliant Blue R-250 (Biorad), Methanol (Merck), Glacial acetic acid (Merck), and distilled water. The following reagents and materials were used for Western blotting, and ELISA analyses: polyvinylidene difluoride (PVDF) membrane, transfer buffer, blocking buffer (5% skim milk in PBS), phosphate-buffered saline (PBS), PBS containing 0.05% Tween-20 (PBST), primary antibody, alkaline phosphatase (AP)-conjugated secondary antibody, pNPP substrate, BCIP-NBT substrate, 3 N Sodium Hydroxide, stop solution, and 96-well ELISA microplates (NEST Scientific).

Histopathological preparation employed 10% neutral in buffered formalin (NBF), graded ethanol series (Supelco, CAS No. 64-17-5), xylene (Merck, CAS No. 1330-20-7), paraffin embedding medium, hematoxylin, eosin, glass slides, and coverslips. Immunohistochemical analysis used mouse monoclonal anti-CD4 primary antibody (Santa Cruz Biotechnology, Dallas, TX, USA; Cat. No. SC-19641), Goat anti-Rabbit IgG–Biotin Conjugate secondary antibody (Sigma-Aldrich, USA; Cat. No. 21537), streptavidin–horseradish peroxidase (SA-HRP), 3,3′-diaminobenzidine (DAB) substrate kit (ScyTek Laboratories, Logan, UT, USA; Cat. No. AKC080), and Mayer's hematoxylin counterstain (Sigma-Aldrich, USA; Cat. No. MHS16-500L).

2.2 Serum Collection

Human serum samples were obtained from nine clinically diagnosed hypothyroid patients through collaboration with Saiful Anwar General Hospital, Malang, Indonesia. Anti-thyroid peroxidase (anti TPO) antibody levels were first quantified individually using the AccuBind Anti-TPO ELISA kit according to the manufacturers instructions. Subsequently, proteins were isolated individually from each serum sample, without pooling, using phosphate-buffered saline containing Tween20 (PBST) supplemented with phenylmethylsulfonyl fluoride (PMSF) as a protease inhibitor. The concentration of the isolated protein fractions was initially estimated using NanoDrop spectrophotometry and subsequently confirmed using the Biuret assay. Based on the combined evaluation of total protein concentration determined by the Biuret assay and anti-TPO antibody levels, serum samples exhibiting relatively high values for both parameters were selected for further characterization. The isolated protein fractions were analyzed by SDS-PAGE followed by silver staining. The protein band at approximately 50 kDa was subsequently recovered by electroelution and used for Western blot analysis, Fourier-transform infrared (FTIR) spectroscopy, LC-MS/MS analysis, and rabbit immunization for antibody production. Individual TSH, T3, and T4 values were not available because the serum samples were obtained through clinical collaboration after routine clinical diagnosis. Therefore, anti-TPO antibody levels were included as an additional serological characterization of the serum samples. Serum samples were stored at -20C for more than one year prior to analysis. To minimize protein degradation, samples were thawed only once during the protein isolation procedure, and repeated freeze-thaw cycles were avoided before subsequent analyses.

2.3 TPO Isolation

Thyroid peroxidase (TPO) was isolated from the sera of hypothyroid patients using a modified protein precipitation and electroelution method based on previous protocols. Briefly, serum samples were mixed with phosphate-buffered saline containing Tween 20 and phenylmethylsulfonyl fluoride (PBST-PMSF) to maintain protein stability and inhibit proteolytic degradation during the isolation process. The mixture was homogenized and subjected to sonication, followed by centrifugation to separate the soluble protein fraction from insoluble components. The resulting supernatant was collected and treated with cold ethanol to precipitate serum proteins. The mixture was incubated under cold conditions and subsequently centrifuged to obtain the protein pellet. The pellet was air-dried to remove residual ethanol and then resuspended in Tris-HCl buffer (pH 6.8). Protein concentration was measured using a NanoDrop spectrophotometer (Thermo Scientific, USA) prior to electrophoretic analysis (Aulanni'am, 2023; Aulanni'am et al., 2018). Total protein was determined using the conventional Biuret method. The Biuret reagent was prepared by dissolving 0.325 g $CuSO_4{\cdot}5H_2O$, 0.902 g potassium sodium tartrate, and 2.4 g NaOH in distilled water and adjusting the final volume to 100 mL. Serum (5 μL) was mixed with 95 μL of Biuret reagent, incubated at room temperature for 30 min, and the absorbance was measured at 540 nm using a UV - Visible spectrophotometer against a reagent blank. Total protein concentration was calculated using a bovine serum albumin (BSA) standard curve and expressed as mg/mL (Aulanni'am, 2023; Rose et al., 2016). Protein separation was performed using sodium dodecyl sulfate polyacrylamide gel electrophoresis (SDS-PAGE) under reducing conditions, employing a 12% resolving gel and a 5% stacking gel. Prior to electrophoresis, protein samples were mixed with loading buffer containing sodium dodecyl sulfate (SDS) and β-mercaptoethanol, followed by heat denaturation at 94°C for 5 min. Electrophoresis was conducted at a constant voltage (150 V) until optimal protein separation was achieved. A prestained protein ladder was included to estimate molecular weight. Following separation, protein bands were visualized using silver staining due to its high sensitivity for detecting low-abundance serum proteins, particularly relevant for targets such as thyroid peroxidase (TPO) (Azzahra et al., 2025; Fiqriyana et al., 2013; Loi Julia and Gam, 2020).

The silver staining procedure consisted of fixation of the gel in a solution containing 40% ethanol, 10% glacial acetic acid, and distilled water for 45 min, followed by washing with distilled water for 30 min. Protein sensitization was performed using 0.02% sodium thiosulfate ($Na_2S_2O_3{\cdot}5H_2O$) for 15 min, followed by a brief wash with distilled water for 1 min. The gel was then equilibrated in 0.1% silver nitrate ($AgNO_3$) solution for 15 min and washed again with distilled water for 1 min. Protein bands were developed using a solution containing 3% sodium carbonate (Na_2CO_3) and 0.05% paraformaldehyde for less than 1 min until clear band visualization was achieved. The staining reaction was terminated and the gel was preserved in 1% acetic acid (Hempelmann and Krafts, 2017; Huang et al., 2018). To confirm the identity of TPO, proteins were transferred from the SDS-PAGE gel onto a nitrocellulose membrane using a wet transfer system for Western blot analysis. The membrane was incubated with monoclonal anti-TPO primary antibody followed by AP-conjugated secondary antibody to detect immunoreactive protein bands. A distinct band at approximately 50 kDa was identified as the target TPO fraction. The confirmed 50 kDa protein band was excised from the gel and purified using an electroelution system (Bio-Rad, USA). The electroelution process was performed using the sample with the highest protein concentration to maximize protein recovery and ensure sufficient yield for downstream analyses. The electroeluted fraction was further precipitated using cold ethanol, frozen, centrifuged, and the resulting pellet was resuspended in Tris-HCl buffer (pH 6.8) (Aulanni'am, 2023). The protein concentration of the final isolated protein fraction was determined after completion of the isolation workflow, including SDS-PAGE, electroelution, ethanol precipitation, and protein resuspension, using the Biuret method. Protein quantification was performed to confirm the availability of sufficient protein for downstream characterization and immunization. Protein concentration was not measured after each interme-

diate purification step; therefore, purification efficiency and protein recovery at individual stages, including electroelution, were not determined.

2.4 TPO Characterizations

2.4.1 Functional Group Analysis Using ATR-FTIR

Functional group analysis of the isolated 50 kDa thyroid peroxidase (TPO) fraction was performed using Fourier Transform Infrared (FTIR) spectroscopy with an ATR module (Shimadzu IRSpirit-T, Japan). The liquid sample was directly applied onto the ATR crystal using a micropipette until the crystal surface was completely covered, followed by gentle pressure to ensure optimal contact. Spectra were recorded in the range of 4000–400 cm^{-1} with a resolution of 4 cm^{-1} and 10 scans per measurement using Happ-Genzel apodization. Background spectra were collected prior to each measurement under identical conditions. After analysis, the ATR crystal was cleaned with ethanol and dried before the next sample measurement. Peak identification and baseline correction were performed using the instrument software, and characteristic absorption bands were interpreted based on standard infrared reference data (Panjaitan et al., 2025).

2.4.2 Amino Acid Composition Analysis Trought LCM-S/MS

The amino acid composition of the isolated 50 kDa thyroid peroxidase (TPO) fraction was analyzed using liquid chromatography–tandem mass spectrometry (LC-MS/MS). Briefly, 0.5 g of the isolated protein sample was hydrolyzed with 10 mL of 6 N HCl and 10 mL of 4 N NaOH, followed by microwave digestion at 195C for 30 min. The hydrolysate was cooled to room temperature, filtered, neutralized to approximately pH 7, diluted with 0.1 N HCl, and passed through a 0.22 μm syringe filter prior to injection. Chromatographic separation was performed using an Intrada Amino Acid column (50 mm × 3 mm) with a mobile phase consisting of solvent A (0.3% formic acid in acetonitrile) and solvent B (acetonitrile/100 mM ammonium formate, 20:80, v/v). A 1 μL sample was injected at a flow rate of 0.6 mL/min with the column temperature maintained at 40°C. Gradient elution was initiated at an A:B ratio of 86:14, increased to 0:100, and then returned to initial conditions for re-equilibration. Mass spectrometric detection was carried out under electrospray ionization conditions with the interface temperature set at 40°C, desolvation temperature at 650°C, DL temperature at 250°C, and heat block temperature at 400°C. Nebulizing gas and drying gas flow rates were maintained at 3 L/min, while heating gas was set at 15 L/min. Amino acid standards were analyzed under identical conditions for calibration and quantitative determination.

2.5 Experimental Design

Male New Zealand White rabbits (Oryctolagus cuniculus), aged 3-4 months and weighing 2.0-2.5 kg, were used in this study. The animals were housed under controlled laboratory conditions with a 12-hour light/dark cycle, temperature of 22-25°C, and relative humidity of 50 - 60%. All rabbits were provided with a standard pellet diet and water ad libitum. Prior to the experiment, the animals underwent a one-week acclimatization period. A total of three rabbits were used (n=3). The treatment group was administered intramuscular injections of TPO emulsified with Freund's adjuvant, consisting of a primary immunization followed by periodic booster injections to induce and sustain an adaptive immune response. Blood samples were collected at regular intervals throughout the study to monitor antibody production. The total duration of the experimental study was 4 months. At the end of the experimental period, all animals were euthanized, and spleen and thymus tissues were collected for histopathological and immunohistochemical analyses to evaluate immune activation and antigen expression. Human serum samples used for TPO isolation were obtained from hypothyroid patients following ethical approval from the Institutional Ethics Committee (Approval No. 187/EC/KEPK/04/2022). All animal procedures were conducted in accordance with institutional and international guidelines for the care and use of laboratory animals and were approved by the Animal Ethics Committee of Brawijaya University (Approval No. 215-KEP-UB-2023).

2.6 TPO Antibody Production

Polyclonal antibody production against the isolated 50 kDa thyroid peroxidase (TPO) fraction was carried out using male New Zealand White rabbits (Oryctolagus cuniculus) aged 3-4 months with body weights of 2.0–2.5 kg. Prior to immunization, 200 μg/mL of purified TPO protein (100 μg per injection) was emulsified with Complete Freunds Adjuvant (CFA) for the first immunization and with Incomplete Freund's Adjuvant (IFA) for booster injections at a 1:1 ratio until a stable emulsion was formed (Delahaut, 2017; Greenfield, 2022). Each rabbit received 500 μL of the antigen-adjuvant emulsion by intramuscular injection into the quadriceps femoris muscle of the hind limb, with injection sites alternated between the left and right legs. The immunization protocol consisted of one primary immunization (week 1) followed by two booster immunizations at weeks 5 and 10, resulting in a cumulative antigen dose of 300 μg per rabbit. This immunization regimen was selected based on established Freund's adjuvant protocols for inducing robust polyclonal antibody responses while minimizing excessive local tissue reactions (Delahaut, 2017; Greenfield, 2022). A pre-immune blood sample was collected before the initial immunization, followed by weekly peripheral venous blood collection from weeks 6 to 14, yielding 10 post-immunization serum samples for monitoring antibody production and subsequent immunoglobulin isolation. For IgG isolation, rabbit serum was mixed with 50% saturated ammonium sulfate (SAS) solution at a 1:1 ratio, vortexed, and centrifuged at 3,000 rpm for 15 min at 4°C. The supernatant was collected and the precipitation step was repeated. The resulting pellet was resuspended and dialyzed overnight in phosphate buffer at 4°C. Ethanol was then added at a 1:1 ratio and the mixture was stored at 4°C for 24 h. After centrifugation, the

supernatant was discarded and the pellet was air-dried to remove residual ethanol before being resuspended in Tris-HCl buffer (pH 6.8). The isolated IgG fraction was used for further immunological analysis (Aulanni'am, 2023).

2.7 Characterization of Anti-rabbit Anti Human TPO

The humoral immune response against the purified 50 kDa TPO protein fragment was evaluated by indirect ELISA. Briefly, the purified antigen was diluted 1:10 in coating buffer, and 50 μL was added to each well of a 96-well microplate followed by overnight incubation at 4°C. After washing with PBST, the wells were blocked with 10% (w/v) bovine serum albumin (BSA) in PBS for 2 h at room temperature. Rabbit sera collected before immunization (PI) and after each immunization (B1-B10) were diluted 1:100 in PBS, added to the wells (50 μL/well), and incubated for 2 h at room temperature. Following washing, alkaline phosphatase-conjugated goat anti-rabbit IgG (1:2500 in PBS) was added and incubated for 2 h. After a final washing step, p-nitrophenyl phosphate (pNPP) substrate was added, and the reaction was developed for 30 min in the dark before being stopped with 3 M NaOH. Absorbance was measured at 405 nm using a microplate reader. All samples were analyzed in triplicate, and the results were expressed as mean ± standard deviation (SD). Protein separation was performed using SDS-PAGE under both reducing and non-reducing conditions using a 12% resolving gel and a 5% stacking gel. Purified IgG samples were mixed with SDS loading buffer either containing β-mercaptoethanol (reducing condition) or lacking β-mercaptoethanol (non-reducing condition). Samples under reducing conditions were heated at 94°C for 5 min prior to electrophoresis, whereas samples under non-reducing conditions were prepared without β-mercaptoethanol. Electrophoresis was carried out at a constant voltage of 150 V until optimal protein separation was achieved. A prestained protein molecular weight marker was included for molecular weight estimation. Following electrophoresis, the gels were stained with Coomassie Brilliant Blue (CBB) R-250 and destained with a methanol-acetic acid solution until distinct protein bands were clearly visible (Azzahra et al., 2025; Fiqriyana et al., 2013; Loi Julia and Gam, 2020).

2.8 Preparation of Spleen and Thymus Histopathological

Spleen and thymus tissues were collected from experimental rabbits and immediately fixed in 10% neutral buffered formalin (NBF) for at least 24h to preserve tissue architecture. Fixed tissues were subsequently processed through a graded ethanol series for dehydration, followed by clearing in xylene and infiltration with molten paraffin. The tissues were then embedded in paraffin blocks and sectioned at a thickness of 4 to 5 μm using a microtome. The sections were floated on a warm water bath, mounted onto glass slides, and dried prior to staining. Histological staining was performed using hematoxylin and eosin (H&E) to evaluate general tissue morphology. Stained sections were dehydrated, cleared, and mounted with coverslips for microscopic observation. Histopathological features of the spleen and thymus were examined using a light microscope (Olympus CX31, Japan) and documented for further analysis (Salman et al., 2020; Tuska et al., 2025).

2.9 Immunohistochemistry Method

Immunohistochemical (IHC) analysis was performed to evaluate CD4 expression in spleen tissue and TPO expression in thymus tissue. Paraffin-embedded tissue sections (4–5 μm) were deparaffinized in xylene and rehydrated through a graded ethanol series, followed by rinsing in distilled water. Endogenous peroxidase activity was blocked, and non-specific binding was minimized using a blocking solution for 1 h at room temperature. The sections were incubated with primary antibodies, including mouse monoclonal anti-CD4 (Santa Cruz Biotechnology, Cat. No. SC-19641) at a dilution of 1:1000 for spleen tissue and anti-TPO antibody for thymus tissue, followed by incubation with Goat anti-Rabbit IgG–Biotin Conjugate secondary antibody (Sigma-Aldrich, Cat. No. 21537) at a dilution of 1:2500. Antigen–antibody complexes were visualized using streptavidin–horseradish peroxidase (SA-HRP) and 3,3′-diaminobenzidine (DAB), followed by counterstaining with Mayers hematoxylin. After dehydration, clearing, and mounting, stained sections were examined under a light microscope (Olympus CX31, Japan) for qualitative and quantitative evaluation of antigen expression (Jankovic et al., 2021; Shehata et al., 2019).

Quantitative image analysis was performed using Image Raster software. Tissue sections were examined under a light microscope at × 400 magnification, and for each rabbit, 20 randomly selected, non-overlapping microscopic fields were analyzed. Positively stained cells were identified by the presence of brown 3,3′-diaminobenzidine (DAB) staining and manually counted using the built-in counter tool in Image Raster. The mean number of positively stained cells from the 20 microscopic fields was calculated for each rabbit and expressed descriptively as mean ± standard deviation (SD). Image analysis was performed by a single investigator using identical counting criteria for all tissue sections. Because positive cells were quantified by manual counting rather than automated image thresholding, thresholding parameters were not applicable in the present study.

2.10 Statistical Analysis

All quantitative data are presented as mean ± standard deviation (SD). For serum analyses, each serum sample obtained from a clinically diagnosed hypothyroid patient was considered one biological replicate (n = 9). Total protein concentrations determined by NanoDrop spectrophotometry and the Biuret assay, as well as anti-thyroid peroxidase (anti-TPO) ELISA measurements, were performed in triplicate (technical replicates) for each serum sample, and the average value was used for subsequent analysis.For the animal experiments, each rabbit was considered one biological replicate. Quantitative immunohistochemical and histological measurements were obtained from multiple microscopic fields for each rabbit, and the mean

value for each animal was used as the representative value for analysis. Descriptive statistics were calculated using Microsoft Excel, and graphs were generated using OriginPro (OriginLab Corporation, Northampton, MA, USA). Image-based quantitative analyses were performed using Image Raster software. Because the in vivo study included a limited number of biological replicates, quantitative data were analyzed descriptively and are presented as mean ± SD. No inferential statistical analyses, normality tests, or hypothesis testing were performed. SDS-PAGE, Western blotting, ATR-FTIR spectroscopy, and LC-MS/MS were used for qualitative biochemical characterization and were therefore not subjected to statistical analysis.

2.11 Structural Modeling and Epitope Mapping of Thyroid Peroxidase

The amino acid sequence of human thyroid peroxidase (TPO) was retrieved from the UniProt database (UniProt ID: P07202). Three-dimensional structural modeling was performed using the AlphaFold Protein Structure Database, which predicts protein structures based on deep learning algorithms. The predicted TPO structure was subsequently visualized and analyzed using BIOVIA Discovery Studio 2025 (Dassault Systèmes, France) to examine domain organization and overall structural features. Domain identification was conducted based on sequence annotation and structural alignment, including the myeloperoxidase (MPO)-like domain, complement control protein (CCP)-like domain, epidermal growth factor (EGF)-like domain, transmembrane region, and cytoplasmic tail. Previously reported immunodominant epitopes of TPO, particularly the core epitope region spanning residues 604–609 (ETPDL) and its flanking regions, were mapped onto the predicted three-dimensional structure to evaluate their spatial localization and surface exposure. Structural analysis focused on identifying epitope accessibility, conformational orientation, and potential antigenic regions relevant to antibody binding. Visualization outputs were used to generate structural representations of TPO and its immunodominant epitopes for further interpretation (Aulanni'am et al., 2024; Khairana et al., 2025).

3. RESULT AND DISCUSSTION

3.1 Characterization of Hypothyroid Patient Serum by Anti-TPO Antibody and Protein Concentration Analysis

To initially characterize the autoimmune status of the hypothyroid patient sera, anti-thyroid peroxidase (anti-TPO) antibody concentrations were determined using the AccuBind Anti-TPO ELISA kit (Figure 1). The ELISA results demonstrated substantial variation among the analyzed serum samples, with antibody concentrations ranging from approximately 20 IU/mL to more than 600 IU/mL. According to the manufacturer's reference criteria, anti-TPO concentrations exceeding 40 IU/mL are considered positive. Accordingly, most serum samples analyzed in the present study were classified as positive, indicating the presence of circulating autoantibodies directed against thyroid peroxidase. The variability in antibody concentrations is consistent with the heterogeneous nature of autoimmune thyroid disease (AITD), in which the magnitude of the humoral immune response differs among individuals. Variations in antibody titers may be influenced by disease stage, duration of autoimmune activity, immune regulation, and differences in B-cell activation and clonal expansion among patients (Caturegli et al., 2014; Ferrari et al., 2017).

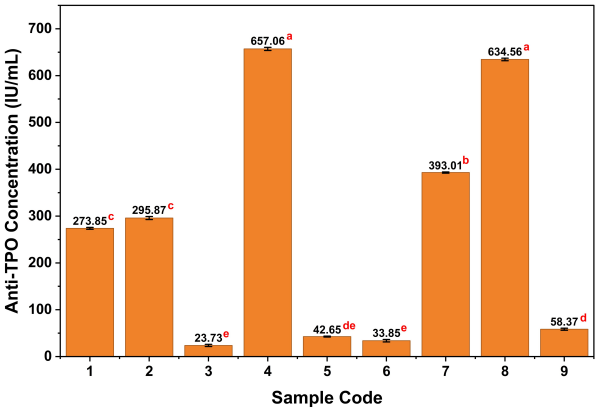

Figure 1. Anti-Tpo Concentration of Hypothyroid Patients Serum

Following serological characterization, the concentration of proteins isolated from the sera of hypothyroid patients was determined using NanoDrop spectrophotometry (Figure 2a) and subsequently confirmed by the Biuret assay (Figure 2b), a colorimetric method that is more specific for total protein quantification. Both analytical methods demonstrated comparable protein concentration profiles across all analyzed samples, with sample 4 consistently exhibiting the highest protein concentration, whereas sample 9 showed the lowest. Although the protein concentrations determined by NanoDrop were slightly lower than those obtained by the Biuret assay, both methods displayed similar trends across the serum samples, indicating good agreement in the relative distribution of protein concentrations.

The differences observed between the two methods are expected because the Biuret assay quantifies proteins based on the formation of copper-peptide complexes under alkaline conditions, whereas NanoDrop spectrophotometry estimates protein concentration by measuring ultraviolet absorbance at 280 nm, which primarily depends on the abundance of aromatic amino acid residues, particularly tryptophan and tyrosine, and may also be influenced by nucleic acids and other ultraviolet-absorbing compounds. Therefore, the Biuret assay was selected as the reference method for quantitative analysis because it is relatively less susceptible to interference from non-protein components. Protein concentrations determined by the Biuret assay ranged from 38.61 ± 0.60 mg/mL to 65.13 ± 0.40 mg/mL, indicating inter-individual variation in the amount of isolated serum protein fractions.

The observed variation in protein concentration may reflect differences in the total amount of proteins recovered from

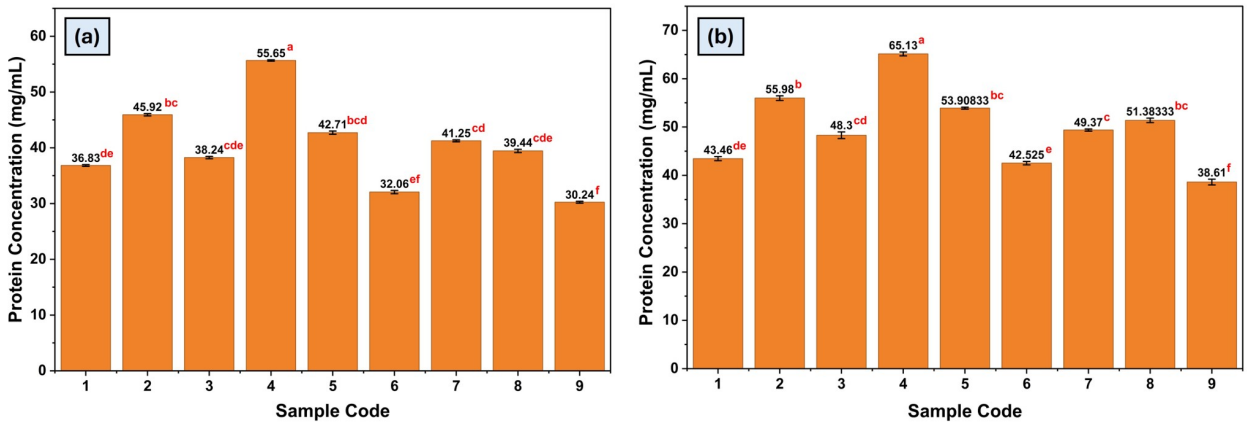

Figure 2. Concentration of Proteins Isolated From the Sera of Hypothyroid Patients Using Nanodrop Spectrophotometry (A) and Subsequently Confirmed by the Biuret Assay (B).

individual serum samples. Human serum is a highly complex biological matrix containing abundant plasma proteins together with lower-abundance tissue-derived proteins released into the circulation under both physiological and pathological conditions (Anderson and Anderson, 2002; Geyer et al., 2017). In autoimmune thyroid disease, damage to thyroid follicular cells has been reported to facilitate the release of thyroid-associated proteins, including thyroid peroxidase (TPO), into the circulation. Nevertheless, because the protein fraction in the present study was isolated directly from serum, it most likely represents a heterogeneous mixture of circulating proteins rather than purified TPO alone. Therefore, the measured protein concentrations should be interpreted as representing the total amount of isolated serum protein rather than the concentration of thyroid peroxidase specifically (Ferrari et al., 2021; Ragusa et al., 2019).

Because the Biuret assay measures total protein concentration whereas ELISA specifically detects circulating anti-TPO antibodies, these two analytical methods provide complementary rather than equivalent information. Total protein concentration reflects the overall quantity of proteins isolated from serum, whereas anti-TPO ELISA reflects the magnitude of the humoral autoimmune response directed against thyroid peroxidase. Therefore, serum samples selected for subsequent analyses were chosen based on the combined evaluation of both parameters. Samples exhibiting relatively high total protein concentrations together with elevated anti-TPO antibody levels were selected for further protein isolation and characterization because they were expected to provide sufficient protein yield while representing sera with high immunoreactivity. This selection strategy was intended to maximize the likelihood of recovering immunoreactive protein fractions suitable for subsequent immunization and immunological characterization (McLeod and Cooper, 2012; Ragusa et al., 2019).

Although elevated anti-TPO antibody concentrations indicate the presence of thyroid-directed autoimmunity, they do not provide evidence regarding the molecular identity or abundance of the isolated protein fraction. Likewise, the Biuret assay provides information only on total protein concentration and cannot distinguish thyroid peroxidase from other serum proteins. Therefore, further characterization was performed using SDS-PAGE, electroelution, Western blotting, Fourier-transform infrared (FTIR) spectroscopy, and LC-MS/MS to evaluate the biochemical characteristics and immunological properties of the isolated protein fraction. The combination of these complementary analytical techniques provides a more comprehensive characterization of the isolated protein than could be achieved by protein quantification or serological analysis alone.

3.2 TPO Molecular Weight Analysis

Molecular weight analysis using SDS-PAGE followed by silver staining revealed a distinct and reproducible protein band at approximately 50 kDa across hypothyroid serum samples (Figure 3). The use of silver staining enabled sensitive detection of low-abundance proteins, which is particularly advantageous for serum-derived proteins. The relatively discrete band pattern with minimal background smearing suggests that the isolation procedure reduced interference from non-specific serum proteins, although it does not demonstrate complete purification.

The observed molecular weight of approximately 50 kDa is lower than that of the full-length native thyroid peroxidase (TPO), which has a reported molecular mass of approximately 100–110 kDa (McLeod and Cooper, 2012). This finding indicates that the isolated protein fraction differs in molecular weight from the native TPO protein. The reduced molecular weight may reflect a processed or truncated protein species; however, it may also result from protein degradation or other events occurring during sample preparation. Previous studies have reported the presence of immunoreactive TPO fragments under certain experimental and pathological conditions (Weetman, 2021; Antonelli et al., 2015). However, because peptide-

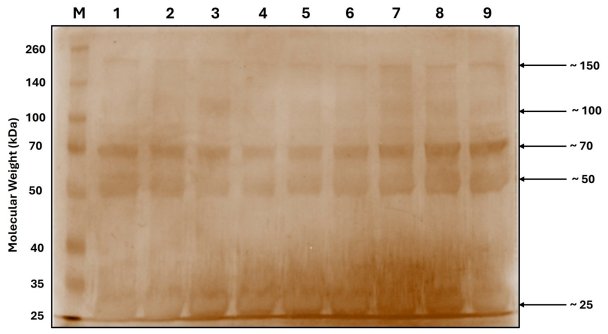

Figure 3. Serum Protein Sample Profile Using 12% Acrylamide Gel Electrophoresis With Silver Staining. M = Marker; 1-9 = Hypothyroid Samples.

level protein identification was not performed in the present study, the molecular origin of the isolated protein fraction cannot be determined from molecular weight analysis alone.

The approximately 50 kDa protein band was selected for further characterization because it consistently appeared as a distinct band in the SDS-PAGE profiles of the selected hypothyroid serum samples. Furthermore, previous Western blot analysis performed by our group demonstrated that this band exhibited immunoreactivity toward an anti-TPO antibody (Ramadani et al., 2024). Accordingly, subsequent biochemical characterization focused on this reproducibly detected immunoreactive protein fraction rather than the native full-length TPO (100-110 kDa). This experimental approach was intended to characterize the isolated immunoreactive protein fraction observed in patient serum rather than to investigate the intact TPO molecule. Nevertheless, because peptide-level protein identification was not performed, the precise molecular origin and physiological relevance of the isolated protein fraction remain to be established.

Because human serum contains abundant proteins, particularly albumin and immunoglobulins, that may migrate within overlapping molecular-weight ranges during SDS-PAGE, molecular weight alone was not considered sufficient to assign the identity of the isolated protein fraction. Therefore, interpretation of the approximately 50 kDa band was supported by complementary analyses, including previously reported Western blot analysis using an anti-TPO antibody (Ramadani et al., 2024). ATR-FTIR characterization, LC-MS/MS amino acid profiling, and evaluation of immunogenicity following rabbit immunization. Collectively, these complementary findings increase confidence that the isolated fraction contains an anti-TPO-reactive protein component. However, because definitive peptide sequencing was not performed, the possibility that co-migrating serum proteins contributed to the isolated fraction cannot be completely excluded and should be considered when interpreting the results.

Western blot analysis using a monoclonal anti-TPO antibody, reported previously by our group (Fiqriyana et al., 2013; Ramadani et al., 2024). demonstrated the presence of an immunoreactive band at approximately 50 kDa. Since these data have been published previously, the present study focuses on further biochemical characterization and evaluation of the biological properties of the isolated protein fraction rather than repeating the same experiment. The observed immunoreactivity supports the interpretation that the isolated protein fraction contains an anti-TPO-reactive component under the experimental conditions employed. However, the present study did not determine whether the isolated protein corresponds to a specific structural domain or immunodominant epitope of TPO.

A methodological limitation of the present study is that protein concentration was quantified only before protein isolation and after completion of the entire isolation workflow, including SDS-PAGE, electroelution, ethanol precipitation, and protein resuspension. Consequently, protein recovery and purification efficiency at individual purification steps could not be determined.

3.3 Functional Group Analysis using ATR-FTIR

The functional group characterization of the isolated 50 kDa thyroid peroxidase (TPO) fraction was performed using ATR-FTIR spectroscopy (Figure 4 and Table 1) to evaluate its chemical composition and structural integrity. The obtained spectrum exhibited several characteristic absorption bands corresponding to proteinaceous and glycoprotein features, confirming the biochemical nature of the isolated fraction.

A broad absorption band observed at approximately 3327 cm^{-1} was attributed to overlapping O–H and N–H stretching vibrations, which are commonly associated with hydrogen-bonded hydroxyl groups and peptide backbone amide groups. This absorption band is consistent with the presence of protein-associated functional groups and hydrogen bonding commonly observed in proteins (Rothschild, 2016; Tatulian, 2019). The broadness of this band may also reflect the presence of polar amino acid residues. Although thyroid peroxidase (TPO) is a glycoprotein, ATR-FTIR alone cannot confirm the presence or extent of protein glycosylation.

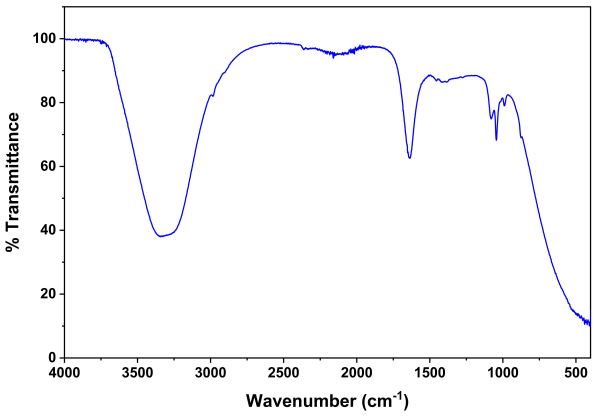

Figure 4. Functional Group Analysis Using Atr-Ftir of Tpo.

Table 1. Sructural Interpretation of TPO Based on Figure 4

Wavenumber (cm^{-1})	Tentative assignment	Structural interpretation	References
3327	O–H and N–H stretching	Hydrogen-bonded hydroxyl groups and peptide backbone amide groups commonly observed in proteins	(Rothschild, 2016; Tatulian, 2019)
1640	Amide I (C=O stretching)	Characteristic protein peptide backbone; commonly associated with general secondary structural elements	(Tintor et al., 2024)
1079	C–O stretching	Carbohydrate-related or alcohol functional groups commonly detected in proteins/glycoproteins	(Tatulian, 2019)
1045	C–O stretching	Protein-associated carbohydrate functional groups	(Tatulian, 2019)
990	C–H bending / phosphate-related vibration	Minor functional group contribution within the isolated protein fraction	(Rothschild, 2016)

The strong absorption band detected at 1640 cm^{-1} corresponds to the amide I region, which primarily arises from C=O stretching vibrations of the peptide backbone. This band is widely recognized as a characteristic feature of proteins and is commonly associated with general secondary structural elements, including contributions from α-helical and β-sheet conformations (Tintor et al., 2024). The presence of a distinct amide I band supports the proteinaceous nature of the isolated fraction and indicates that characteristic peptide backbone structures remained detectable following the isolation procedure. However, ATR-FTIR alone cannot determine the preservation of native protein conformation, conformational epitopes, or antigenicity.

Additional absorption bands observed in the fingerprint region, particularly at approximately 1079 and 1045 cm^{-1}, correspond to C–O stretching vibrations (Tatulian, 2019). These bands may be associated with carbohydrate-related functional groups that are commonly detected in glycoproteins. However, these spectral features should not be interpreted as direct evidence of glycosylation because ATR-FTIR does not provide sufficient structural specificity for this purpose.

A weaker absorption band detected around 990 cm^{-1} may be attributed to out-of-plane C–H bending vibrations or phosphate -related functional groups. Although less pronounced, this band may reflect minor chemical components present within the isolated protein fraction. Overall, the ATR-FTIR spectrum is consistent with the presence of characteristic protein-associated functional groups and provides complementary biochemical information regarding the isolated protein fraction (Rothschild, 2016; Tatulian, 2019). These findings, the ATR-FTIR spectrum is consistent with the presence of characteristic protein-associated functional groups and provides complementary biochemical information regarding the isolated protein fraction. Together with SDS-PAGE, and LC-MS/MS analyses, the ATR-FTIR findings contribute to the overall characterization of the isolated protein used in this study.

3.4 Amino Acid Composition Analysis (LC-MS/MS)

The isolated protein fraction was analyzed by LC–MS/MS following complete acid hydrolysis to determine its amino acid composition as part of its biochemical characterization (Crotty, 2019). The analysis detected several amino acids, including L-arginine, L-cystine, L-glutamic acid, L-histidine, L-isoleucine, L-leucine, L-lysine, L-phenylalanine, L-proline, and L-threonine, with concentrations ranging from 1.233 to 2.013 nmol/mL (Table 2). These amino acids were detected with well-resolved retention times, indicating satisfactory chromatographic separation and reliable analytical performance under the applied analytical conditions.

The detected amino acid profile confirms that the isolated fraction is proteinaceous and provides complementary biochemical information regarding its composition. Among the identified amino acids, cystine is particularly relevant because it participates in disulfide bond formation, which contributes to the structural stability of many proteins. Likewise, aromatic amino acids such as phenylalanine and histidine, together with charged residues including arginine, lysine, and glutamic acid, are common constituents of proteins involved in protein folding, intermolecular interactions, and structural organization (Zhu, 2018; Akbar et al., 2022). In addition, hydrophobic amino acids such as leucine, isoleucine, and proline contribute to hydrophobic core formation and conformational stability, while proline plays an important role in stabilizing structural turns within protein molecules (Finkelstein, 2018; Benlaribi et al., 2022). Several amino acids commonly found in proteins, including methionine, valine, tyrosine, tryptophan, and aspartic acid, were not detected or were present below the limit of quantification. This incomplete amino acid recovery may result from degradation of acid-labile residues during hydrolysis, incomplete hydrolysis, or analytical detection limitations. For example, tryptophan and methionine are known to undergo degradation under strong acidic hydrolysis conditions, whereas the responses of several amino acids may be influenced by differences in ionization efficiency during LC–MS/MS analysis (Liu et al., 2019; Rehlund et al., 2025).

It should be emphasized that the LC–MS/MS analysis per-

Table 2. Amino Acid Composition in Tpo Protein Analysis Using Lc-Ms/ms

Amino Acid	Retention Time	Conc. (nmol/mL)
L-Arginine	10.948	1.692
L-Cystine	7.770	1.542
L-Glutamic Acid	6.595	1.812
L-Histidine (Event 7)	9.829	1.233
L-Isoleucine	4.212	1.881
L-Leucine	3.985	1.790
L-Lysine HCl	10.491	1.439
L-Phenylalanine	3.869	1.907
L-Proline	4.493	1.988
L-Threonine	6.593	2.013
L-Histidine (Event 19)	9.857	1.496

formed in the present study was designed to determine amino acid composition after complete hydrolysis rather than to identify peptide sequences. Consequently, the obtained data cannot be used to assign protein identity or determine peptide sequence coverage because the original protein structure had been converted into free amino acids prior to analysis. Therefore, the LC–MS/MS results should be interpreted as biochemical characterization of the isolated protein fraction rather than definitive molecular identification of thyroid peroxidase (TPO) (Kaspar et al., 2009; Noor et al., 2021).

The amino acid composition nevertheless complements the biochemical characterization obtained from SDS-PAGE, Western blot immunoreactivity, and ATR–FTIR analyses by demonstrating that the isolated approximately 50 kDa fraction contains protein-derived constituents. Collectively, these analytical approaches provide evidence that the isolated material is a proteinaceous fraction exhibiting anti-TPO immunoreactivity under the experimental conditions employed. However, definitive confirmation of its molecular identity would require bottom-up proteomic analysis using enzymatic digestion followed by LC–MS/MS peptide mapping against the human TPO sequence, allowing identification of unique peptides and determination of sequence coverage (Gessulat et al., 2019; Noor et al., 2021). Amino acid composition analysis demonstrates that the isolated 50 kDa fraction possesses the biochemical characteristics of a protein and provides complementary information regarding its molecular composition. Because peptide sequencing was not performed, the present findings should not be interpreted as definitive identification of TPO but rather as biochemical characterization of an isolated anti-TPO-reactive protein fraction suitable for subsequent immunogenicity evaluation.

3.5 Production and Characterization of Anti Rabbit Anti Human TPO

The results of the indirect ELISA showed that the isolated 50 kDa TPO protein was capable of inducing a specific humoral immune response in rabbits. Pre-immunization (PI) serum had a low absorbance value (OD_{405} = 0.152), indicating the absence of detectable TPO antibody prior to immunization. After immunization, anti-TPO IgG levels increased significantly, especially after the booster immunization, and continued to rise until reaching the highest absorbance value at the 8th blood draw (B8) with an OD_{405} of 0.555. Although there was a slight decrease in anti-TPO IgG levels at blood draws B9 and B10, the values remained higher than those in the pre-immunization serum until the end of the observation period, as shown in Figure 5.

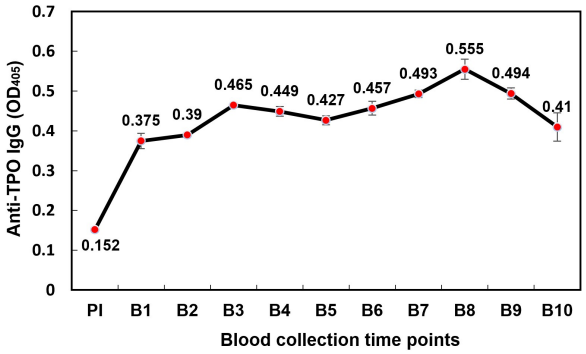

Figure 5. Anti-Tpo Igg Response in Rabbits Immunized With the Isolated 50 Kda Tpo Protein, Determined by Indirect Elisa. Anti-Tpo Igg Levels Are Expressed as Od_{405} (N = 3). Pi = Pre-Immune; B1–b10 = Post-Immunization Blood Collections.

The increase in antibody levels after primary immunization reflects the initiation of the adaptive immune response. During this phase, B cell recognize the administered antigen through their B-cell receptors (BCRs), undergo activation with the assistance of $CD4^+$ T helper cells, and subsequently differentiate into antibody-secreting plasma cells and memory B cells (Suan et al., 2017; Weisel and Shlomchik, 2017). Because primary immune responses require antigen processing, antigen presentation, and lymphocyte activation, antibody production

generally develops gradually before reaching detectable levels. Similar increases in antigen-specific antibody responses following immunization have also been reported in experimental animal models, including oral immunization with recombinant Lactococcus lactis, which induced enhanced humoral immune responses accompanied by increased IgG production (Nugroho et al., 2026).

Administration of booster immunizations using Incomplete Freund's Adjuvant (IFA) further enhanced the antibody response, resulting in higher anti-TPO IgG levels than those observed after the primary immunization. This enhanced response is characteristic of secondary humoral immunity, in which previously generated memory B cells are rapidly reactivated upon re-exposure to the antigen. Consequently, memory B cells proliferate and differentiate into plasma cells more efficiently, leading to increased antibody production. In addition to increasing antibody quantity, secondary immune responses are generally associated with affinity maturation, producing antibodies with improved antigen-binding affinity (Carter et al., 2017). The highest anti-TPO IgG level was observed at blood collection point B8, followed by a slight decline at B9 and B10. This decrease is consistent with the contraction phase of the adaptive immune response that normally occurs after peak antibody production has been achieved. As antigenic stimulation diminishes, a proportion of short-lived plasma cells undergo apoptosis, resulting in a gradual reduction in circulating antibody levels. Nevertheless, anti-TPO IgG levels remained substantially higher than those measured prior to immunization throughout the observation period, indicating the persistence of the humoral immune response induced by the isolated protein fraction (Zhang et al., 2007).

The relatively stable antibody levels observed after repeated booster immunizations also suggest sustained stimulation of the adaptive immune system throughout the immunization period. Although minor fluctuations in antibody concentration were observed between sampling time points, the overall response remained consistently elevated compared with pre-immunization serum. Such variations are commonly observed in polyclonal antibody production and may reflect individual differences in immune regulation, antigen processing, and the dynamic balance between antibody production and natural immunoglobulin turnover (Uhlén et al., 2016; Weisel and Shlomchik, 2017).

It should be noted that the indirect ELISA results demonstrate the ability of the isolated protein fraction to induce antigen-reactive antibody production under the experimental conditions used in this study. However, ELISA alone does not establish the molecular identity of the immunizing antigen or confirm that the generated antibodies specifically recognize thyroid peroxidase (TPO). Therefore, further biochemical characterization by SDS-PAGE and immunoreactivity assessment by Western blot analysis were performed to further characterize the isolated protein fraction and the antibodies generated following immunization. The purified rabbit IgG fraction was characterized by SDS-PAGE under both non-reducing and reducing conditions to evaluate its structural integrity prior to immunoblotting analysis (Figure 6). Under non-reducing conditions, a predominant protein band was observed at approximately 150 kDa, corresponding to intact IgG. Because the interchain disulfide bonds remained intact under these conditions, the antibody migrated as a complete immunoglobulin molecule composed of two heavy chains and two light chains linked through disulfide bridges. The predominance of a single protein band at the expected molecular weight indicates that the purification procedure successfully preserved the native structural organization of rabbit IgG (Khairana et al., 2025).

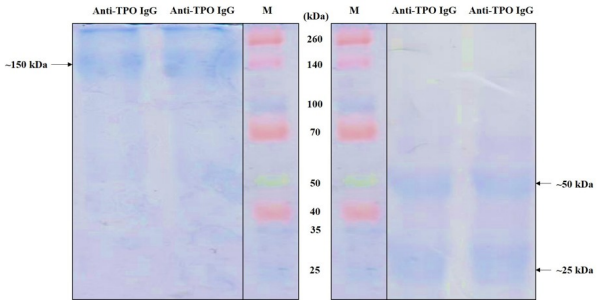

Figure 6. Sds-Page Analysis of the Purified Rabbit Igg Fraction Under Non-Reducing (Left) and Reducing (Right) Conditions. M : Protein Molecular Weight Marker.

Following reduction with β-mercaptoethanol, the purified IgG fraction separated into two characteristic protein bands with molecular weights of approximately 50 kDa and 25 kDa, corresponding to the heavy and light chains of IgG, respectively. The appearance of these expected electrophoretic bands confirms that the reducing conditions efficiently disrupted the interchain disulfide bonds while preserving the individual polypeptide chains. This electrophoretic pattern is consistent with the well-established structural organization of mammalian IgG and has been widely reported as an indicator of antibody integrity following purification (Makaraviciute et al., 2016).

Comparison of the reducing and non-reducing electrophoretic profiles provides additional evidence supporting the successful purification of the rabbit IgG fraction. Under non-reducing conditions, the antibody remained predominantly in its intact form, whereas reduction produced the characteristic heavy and light chain bands expected for purified IgG. Moreover, only minimal additional protein bands were observed in either electrophoretic condition, suggesting that the purification procedure generated a relatively enriched IgG fraction with limited detectable contamination from other serum proteins. Although SDS-PAGE alone cannot determine antibody purity quantitatively, the observed electrophoretic profile indicates that the isolated antibody preparation was suitable for subsequent immunological analysis (Kirley and Norman, 2018; Mariam et al., 2026).

Characterization of the purified antibody prior to immunoblotting is important because residual serum proteins, particularly albumin and other abundant plasma proteins, may interfere

with downstream antibody-based assays if not adequately removed. Therefore, confirmation of the expected IgG electrophoretic profile increases confidence that the immunoreactive signals observed in the subsequent Western blot analysis originated predominantly from antigen-specific IgG generated following immunization rather than from nonspecific serum components (Mariam et al., 2026).

However, SDS-PAGE provides information primarily on molecular weight and structural integrity and does not directly evaluate antibody affinity or antigen specificity. Consequently, the functional performance of the purified antibody was subsequently assessed by Western blot analysis using the isolated protein fraction as the target antigen. The combined electrophoretic characterization and immunoblotting results therefore provide complementary evidence supporting the suitability of the purified rabbit IgG for downstream immunological applications (Ghosh et al., 2014; Mariam et al., 2026).

To further evaluate the immunoreactivity of the generated polyclonal antibodies, Western blot analysis was performed using immune rabbit serum as the primary antibody. As shown in Figure 7, a distinct immunoreactive band was detected at approximately 50 kDa, whereas no corresponding signal was observed in the secondary antibody-only control. This finding indicates that the detected signal depended on the presence of antibodies generated following immunization rather than nonspecific binding of the secondary antibody. The absence of detectable immunoreactivity in the negative control therefore supports the specificity of the antigen-antibody interaction under the experimental conditions employed.

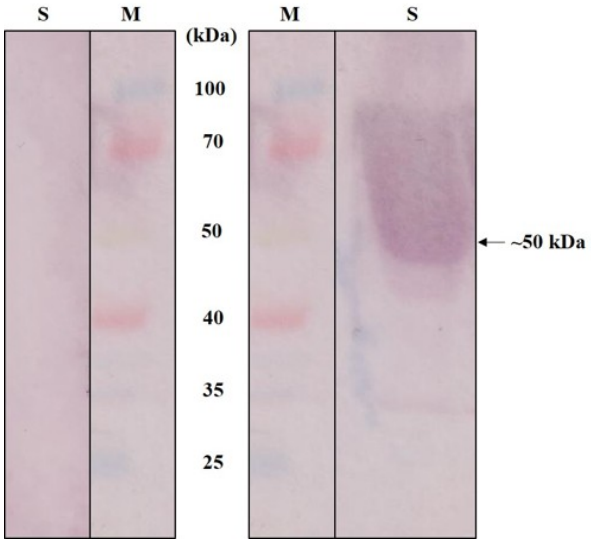

Figure 7. Western Blot Analysis of the Isolated 50 Kda Tpo Protein. Left: Secondary Antibody-Only Control; Right: Rabbit Anti-Human Tpo (Primary Antibody). M: Protein Molecular Weight Marker, S: Sample.

The molecular weight of the detected immunoreactive band corresponded to the protein fraction previously isolated by SDS-PAGE and electroelution. The consistent detection of an approximately 50 kDa protein throughout the isolation, purification, and immunoblotting procedures indicates that this protein fraction retained antibody-reactive properties following purification. Rather than relying solely on molecular weight, the Western blot results provide immunological evidence that the isolated protein fraction contains antigenic determinants recognized by antibodies generated after rabbit immunization (Ghosh et al., 2014).

These findings are consistent with the overall experimental workflow of the present study. The approximately 50 kDa protein band was first identified as a reproducible band in the SDS-PAGE profiles of selected hypothyroid serum samples and was subsequently isolated for biochemical characterization and immunization. The ability of immune rabbit serum to recognize the same protein fraction on Western blot support the conclusion that the isolated protein was capable of eliciting an antibody response under the experimental conditions used in this study. This observation complements the biochemical characterization obtained by ATR-FTIR and amino acid composition analysis, supporting the conclusion that the isolated fraction represents an immunoreactive protein suitable for antibody production (Weisel and Shlomchik, 2017).

Nevertheless, the present Western blot experiment should be interpreted within the limitations of the study. Although the immune serum recognized the isolated approximately 50 kDa protein fraction, the experiment was designed to evaluate immunoreactivity rather than definitive protein identity. Because peptide-level protein identification was not performed, the precise molecular identity and structural origin of the isolated protein fraction could not be established solely by Western blot analysis. Furthermore, additional validation using purified recombinant TPO, thyroid tissue extracts, or peptide sequencing would further strengthen the characterization of antibody specificity. Therefore, the Western blot findings should be considered complementary evidence supporting the immunoreactivity of the isolated protein fraction rather than definitive proof of its molecular identity (Ghosh et al., 2014).

3.6 Spleen and Thymus Histopathology by Inducing TPO in Rabbit

Histopathological evaluation of the spleen and thymus was performed to assess the systemic immune response induced by the isolated 50 kDa thyroid peroxidase (TPO) antigen (Figure 8). Clear morphological differences were observed between control and TPO-treated groups, indicating that administration of the antigen elicited significant immunological activation affecting both secondary and primary lymphoid organs.

In the spleen, hematoxylin and eosin (H&E) staining revealed an apparent expansion of the white pulp region in TPO-induced rabbits compared with controls. Quantitative morphometric analysis showed a greater mean white pulp diameter in the TPO-induced group (47.81 ± 1.11 µm) than in the control group (36.37 ± 1.45 μm), representing an increase of approximately 31.45%. The white pulp is composed pri-

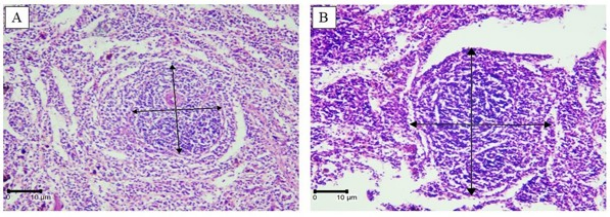

Figure 8. Whistopathology of Rabbit Spleen at 100× Magnification. Control Group (A) and Induced by Tpo Group (B).

marily of periarteriolar lymphoid sheaths (PALS), which are enriched in T lymphocytes, and lymphoid follicles containing B lymphocytes (Lewis et al., 2019; Vancauwenberghe et al., 2015). Enlargement of this region is generally associated with increased lymphoid activity and may reflect enhanced lymphocyte accumulation or proliferation in response to antigenic stimulation. However, the present H&E findings do not allow direct identification of specific lymphocyte subsets or germinal center activity (Stebegg et al., 2018).

The splenic enlargement observed in this study may be related to activation of adaptive immune processes following exposure to the TPO antigen. In secondary lymphoid organs, antigens can be captured and processed by antigen-presenting cells, leading to activation of T and B lymphocytes (Hato et al., 2024; Crotty, 2019). Such immune activation is commonly accompanied by structural changes in lymphoid tissues, including expansion of the white pulp (Lewis et al., 2019; Stebegg et al., 2018). Nevertheless, the current study did not directly evaluate antigen presentation, T-cell activation, B-cell differentiation, or clonal expansion; therefore, these mechanisms should be considered as plausible interpretations rather than demonstrated events.

In the context of autoimmune thyroid disease, sustained exposure to thyroid antigens has been associated with activation of lymphoid tissues and expansion of autoreactive lymphocyte populations The splenic histopathological changes observed in the present study show that administration of the isolated TPO fragment was associated with significant remodeling of the white pulp. These findings support the interpretation that the isolated TPO fragment is capable of eliciting an immune response in vivo. However, further studies incorporating immunophenotyping, cytokine analysis, and antigen-specific antibody measurements are required to determine the specificity and functional characteristics of the induced immune response (Lewis et al., 2019; Stebegg et al., 2018; Weetman, 2021). In parallel, histopathological examination of the thymus revealed distinct structural alterations in TPO-treated rabbits compared to controls (Figure 9). The thymus, as a primary lymphoid organ, plays a central role in T-cell development, selection, and establishment of immune tolerance (Gulla et al., 2023; Miller, 2020). In the TPO-induced group, thymic sections exhibited cortical thinning, reduced lymphocyte density in the cortex, and a less distinct corticomedullary boundary. These changes suggest increased thymocyte turnover and redistribution, likely reflecting heightened immune activation and antigen-driven modulation of T-cell maturation processes (Wang et al., 2015; Weetman, 2021).

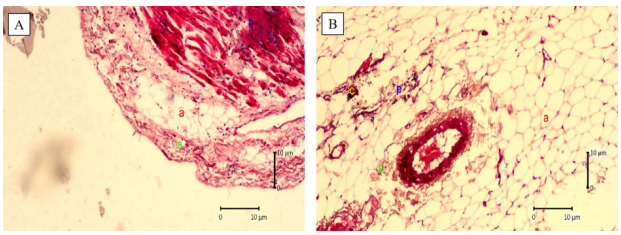

Figure 9. Histopathological Features of Rabbit Thymus Tissue at 100× Magnification. (A) Control Rabbit Thymus Showing Normal Histological Architecture; (B) Thymus Tissue From Rabbit Immunized With 50 Kda Tpo Antigen. Notes: (A) Adipose Tissue, (S) Septa, (P) Parenchyma, and (C) Cystic Structure.

From a mechanistic perspective, the observed thymic remodeling may be associated with changes in immune activity occurring during repeated antigen exposure. Previous studies have suggested that sustained antigenic stimulation can influence thymic architecture by altering the distribution and maturation of thymocytes (Crotty, 2019; Gulla et al., 2023; Miller, 2020). However, because the present study did not assess thymocyte subsets, cellular proliferation, apoptosis, or positive and negative selection processes, no conclusions can be drawn regarding the involvement of central tolerance mechanisms. Further investigations incorporating cellular and molecular analyses will be required to clarify the biological significance of the observed thymic changes. The combined histopathological findings in the spleen and thymus indicate that immunization with the isolated protein fraction was associated with structural changes in both secondary and primary lymphoid organs. Enlargement of splenic white pulp together with alterations in thymic architecture is consistent with activation of immune-associated processes following antigen administration. Although the spleen and thymus serve distinct immunological functions, the concurrent observations in both organs suggest that the isolated protein fraction was capable of eliciting measurable biological responses under the experimental conditions used in this study (Abramson and Anderson, 2017; Lewis et al., 2019).

Taken together with the serological, immunohistochemical, and biochemical findings, the histopathological observations support the immunogenic potential of the isolated protein fraction. Rather than demonstrating the physiological function of a native TPO fragment, these results indicate that the experimentally isolated protein fraction possesses antigenic properties sufficient to induce measurable immune responses in rabbits following immunization. Because peptide-level protein identification was not performed, the precise molecular identity and

structural origin of the isolated protein remain to be established (Ghosh et al., 2014; Zhang et al., 2007).

Overall, the histopathological alterations observed in the spleen and thymus are consistent with immune-associated tissue responses following immunization with the isolated approximately 50 kDa immunoreactive protein fraction. Together with the biochemical and immunological findings, these observations support the immunogenic potential of the isolated protein fraction. However, because peptide-level protein identification was not performed, its precise molecular identity remains to be established.

3.7 CD4$^+$ T Cell Expression in the Rabbit Spleen and TPO 50 kDa Expression in the Rabbit Thymus by Immunohistochemical Technique

Immunohistochemical (IHC) analysis was performed to evaluate the adaptive immune response induced by the isolated 50 kDa thyroid peroxidase (TPO) antigen, focusing on CD4$^+$ T cell expression in the spleen and TPO immunoreactivity in the thymus (Figure 10). The results demonstrated a significant enhancement of immune activation in TPO-treated rabbits compared to controls, providing direct evidence of antigen-driven immunogenicity at both peripheral and central immune sites (Raphael et al., 2020). In the spleen, CD4 immunoreactivity was predominantly localized within the white pulp, particularly in the periarteriolar lymphoid sheath (PALS) and marginal zone, regions that are enriched in T lymphocytes and play important roles in adaptive immune responses. Quantitative image analysis showed a higher mean number of CD4-positive cells in the immunized group (41.25 ± 2.81) than in the control group (31.00 ± 3.59), corresponding to an approximately 33% increase. Although this trend is consistent with enhanced immune-associated cellular responses following immunization, the limited number of biological replicates in the present study precludes formal statistical inference.

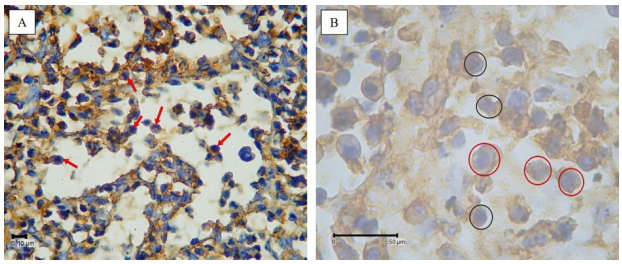

Figure 10. Cd4$^+$ T Expression in Rabbit Spleen Tissue Analyzed by Immunohistochemistry (Ihc) of Control Group (A) and Tpo-Induced Group (B) at 400× Magnification. Red Arrows Indicate Cd4-Positive Expression.

CD4$^+$ T lymphocytes play important roles in coordinating adaptive immune responses by interacting with antigen-presenting cells and supporting B-cell activation through cytokine production and cell-cell interactions (Hirahara and Nakayama, 2016; Ruterbusch et al., 2020). Although the present study did not evaluate CD4$^+$ T-cell subsets or cytokine expression, the increased number of CD4-positive cells observed in the immunized animals is consistent with immune responses following antigen exposure. However, the functional phenotype of these CD4-positive cells, including differentiation into Th1, Th2, Th17, or T follicular helper cells, was not investigated in this study.

Previous studies have demonstrated that CD4$^+$ T cells contribute to humoral immune responses by providing signals required for B-cell activation and antibody production (Raphael et al., 2015; Wang et al., 2015). In the present study, the increased CD4 immunoreactivity was observed together with elevated anti-TPO IgG levels following immunization. Although these findings are consistent with activation of adaptive immune responses, the present study was not designed to establish a direct causal relationship between increased CD4 expression and antibody production.

The localization of CD4-positive cells within the splenic white pulp is also consistent with the histopathological observation of white pulp enlargement following immunization. Because the white pulp is the principal site of antigen presentation and lymphocyte activation in the spleen, the concurrent increase in CD4-positive cells and white pulp expansion suggests that immunization with the isolated protein fraction was associated with structural and cellular changes within this lymphoid compartment (Lewis et al., 2019; Stebegg et al., 2018).

In this study, CD4 immunohistochemistry was used as an early indicator of T helper cell activation following immunization with a 50 kDa isolated TPO protein. CD4 T cells play a crucial role in coordinating the adaptive immune response through B cell activation and antibody production (Crotty, 2019). However, the adaptive immune response involves interactions among various immune cell populations. Previous studies have shown that CD8 T cells contribute to both cellular and humoral immune responses; CD20 reflects B-cell activation; CD68 indicates macrophage involvement in antigen processing and the inflammatory response; and CD86 is an important costimulatory molecule required for optimal T-cell activation (Hammarlund et al., 2017; Klein et al., 2019; Valentine et al., 2018). Therefore, evaluation of these markers will provide a more comprehensive characterization of the immune response induced by the isolated 50 kDa TPO protein. Since this study evaluated only CD4 expression, analysis of these markers should be considered in future research. Although increased CD4$^+$ T-cell expression was observed following immunization, functional characterization of helper T-cell responses through cytokine profiling was beyond the scope of the present study. Cytokines such as interferon-γ (IFN-γ), interleukin-2 (IL-2), interleukin-4 (IL-4), interleukin-17 (IL-17), and tumor necrosis factor-α (TNF-α) are important indicators of T-cell activation and polarization. IFN-γ and IL-2 are commonly associated with Th1-mediated cellular immune responses, whereas IL-4 reflects Th2-mediated humoral immunity by promoting B-cell activation and antibody production. IL-17 is a hallmark cytokine of Th17 cells and has

been implicated in chronic inflammation and autoimmune diseases, including autoimmune thyroid disorders, while TNF-α contributes to inflammatory responses and immune cell recruitment (Bossowski et al., 2013; Raphael et al., 2020; Zhu, 2018). Evaluation of these cytokines would provide additional functional evidence regarding the nature of the immune response elicited by the isolated protein fraction.

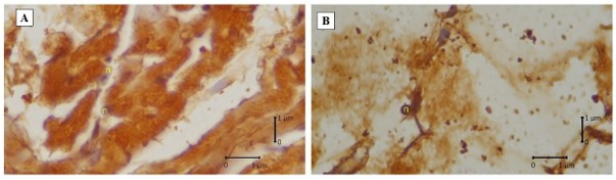

Figure 11. Tpo Expression in Rabbit Thymus of Control Group (A), and Tpo-Induced Group (B) at 400× Magnification. Note: Negative Cells (N).

In parallel, immunohistochemical analysis of thymic tissue demonstrated TPO immunoreactivity exclusively in rabbits immunized with the isolated 50 kDa TPO antigen, whereas no comparable staining was observed in the control group (Figure 11). The immunoreactive signals were predominantly localized within the medullary region of the thymus, particularly in areas exhibiting histological alterations. These findings suggest that the administered TPO antigen or antigen-associated immunoreactive material was detectable within the thymic tissue following immunization (Benlaribi et al., 2022; Yamano et al., 2015).

The thymic medulla is an important microenvironment for antigen presentation during T-cell maturation and central tolerance, where medullary thymic epithelial cells (mTECs) and professional antigen-presenting cells expose developing thymocytes to self-antigens (Yamano et al., 2015). Therefore, the localization of TPO immunoreactivity within this region is consistent with the presence of antigen-associated signals in a compartment involved in thymic antigen presentation. However, the present study did not directly evaluate antigen uptake, processing, or presentation by specific thymic cell populations. Consequently, these findings should be interpreted as supportive evidence of thymic antigen localization rather than direct evidence of antigen processing or central tolerance mechanisms (Abramson and Anderson, 2017; Klein et al., 2019).

Furthermore, although thymic TPO immunoreactivity was detected following immunization, the absence of isotype and negative staining controls limits definitive assessment of staining specificity. Accordingly, the immunohistochemical findings are interpreted conservatively as evidence of TPO-associated immunoreactivity within the thymus. Future studies incorporating appropriate immunohistochemical controls and additional immune cell markers will be required to further characterize the cellular localization and functional significance of the observed staining (Uhlén et al., 2016).

Together with the increased $CD4^+$ T-cell expression observed in the spleen, these findings support the conclusion that immunization with the isolated 50 kDa TPO fragment elicited measurable immune-associated changes in both primary and secondary lymphoid organs. However, the precise cellular mechanisms underlying thymic TPO immunoreactivity require further investigation (Crotty, 2019). From a translational perspective, these findingssupport the potential of the isolated TPO fragment as an immunogen for antibody production. The increased $CD4^+$ T cell expression observed in immunized rabbits is consistent with the estabilished role of helper T cells in supporting adaptive responses (Crotty, 2019). Moreover, the detection of TPO immunoreactivity in the spleen and thymus indicates that the isolated protein remained immunoreactive following the isolation and purification procedures.

Overall, the immunohistochemical findings indicate that immunization with the isolated 50 kDa TPO fragment was associated with increased $CD4^+$ T-cell expression in the spleen and detectable TPO immunoreactivity in the thymus. These observations support the immunogenic potential of the patient-derived TPO fragment and provide a basis for its further evaluation as an immunogen for immunological studies and polyclonal antibody production.

3.8 TPO Structure and Epitope

To facilitate interpretation of the experimental findings, the structural model of TPO and the reported distribution of immunodominant epitopes are presented in Figures 8 and 9. Because peptide-level sequence identification was not performed, the exact structural origin of the isolated ~50 kDa protein fraction could not be determined experimentally. Therefore, Figures 8 and 9 are presented solely to provide structural context based on previously published TPO architecture and epitope mapping, rather than direct evidence for localization of the isolated protein fraction.

The structural organization and epitope distribution of TPO (Figures 12 and 13) are summarized from previous studies to provide a molecular framework for interpreting its immunogenicity and antibody recognition. In silico modeling based on the full-length human TPO sequence revealed a multidomain architecture typical of heme peroxidases, consisting of a large extracellular region, a single transmembrane helix, and a short cytoplasmic tail (McLachlan and Rapoport, 2017; Williams et al., 2020). The extracellular domain is composed of three major structural modules: a myeloperoxidase (MPO)-like catalytic domain, followed by complement control protein (CCP)-like and epidermal growth factor (EGF)-like domains. These domains are stabilized by multiple disulfide bonds, contributing to a rigid and highly ordered three-dimensional conformation (Liu et al., 2016).

The MPO-like domain represents the catalytic core of TPO and contains the heme-binding site essential for iodination and coupling reactions in thyroid hormone synthesis. Structurally, this domain is characterized by a predominantly α-helical fold interspersed with β-sheet regions, forming a compact and enzymatically active structure. Importantly, this domain also

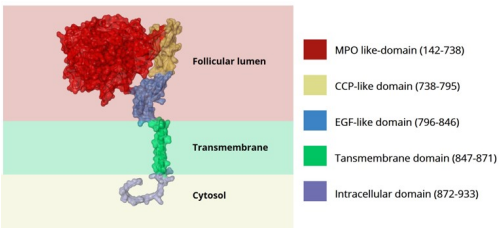

Figure 12. Structure of Thyroid Peroxidase (Tpo).

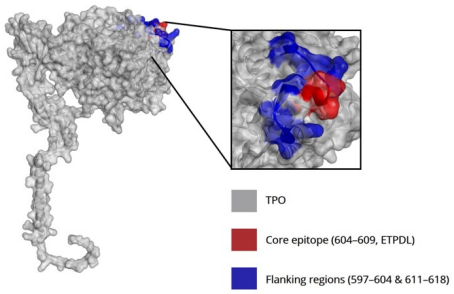

Figure 13. Structural Localization of the Immunodominant Epitope on Tpo.

harbors the majority of immunodominant epitopes recognized by anti-TPO antibodies. Epitope mapping analysis (Figure 13) identified two major immunodominant regions, IDR-A and IDR-B, which are spatially clustered on the surface of the MPO-like domain (McLeod and Cooper, 2012).

These epitopes are predominantly conformational, formed by discontinuous amino acid residues brought into proximity through protein folding. One of the key linear motifs identified within this region is the ETPDL sequence (residues 604–609), which is frequently reported as part of the core epitope. Structural visualization indicates that this region is surface-exposed and located in close proximity to other antigenic residues, forming a contiguous antigenic patch accessible to antibody binding. The surface accessibility of these epitopes is critical, as it enables efficient recognition by circulating anti-TPO antibodies in autoimmune thyroid disease (Aulanni'am et al., 2024; Benvenga and Vita, 2018; Espenbetova et al., 2022) A key structural insight from this analysis is that the immunodominant epitopes are spatially distinct from the catalytic center of the enzyme. This separation suggests that antibody binding does not directly inhibit enzymatic activity through active-site blockage but may instead interfere with protein conformation, stability, or membrane localization. This observation aligns with clinical findings indicating that anti-TPO antibodies are more strongly associated with immune-mediated tissue damage rather than direct enzymatic inhibition (Rapoport and McLachlan, 2018; Weetman, 2021).

The CCP-like and EGF-like domains, although not directly involved in catalysis, contribute to the overall structural stability and may play supportive roles in protein–protein interactions and antigen presentation. These domains also participate in maintaining the conformational integrity required for proper epitope formation. Disruption of these regions, either through proteolytic cleavage or denaturation, may alter epitope presentation and consequently affect antibody recognition. From an immunological perspective, the dominance of conformational epitopes in TPO highlights the importance of preserving three-dimensional structure for accurate antigenicity. Unlike linear epitopes, which are defined by continuous amino acid sequences, conformational epitopes depend on the spatial arrangement of residues within the folded protein (Pedersen and Laurberg, 2009). This explains why recombinant or denatured TPO fragments often exhibit reduced immunoreactivity unless structural integrity is maintained. The discussion of conformational epitopes presented here is based on previously published studies describing TPO antigenicity and is provided to facilitate interpretation of the experimental findings. The present study did not directly evaluate conformational epitope preservation.

Furthermore, the structural localization of epitopes provides insight into the pathogenesis of autoimmune thyroid disease. The exposure of immunodominant regions on the protein surface makes TPO highly susceptible to immune surveillance. Under conditions of thyroid inflammation or cellular damage, these epitopes become more accessible to antigen-presenting cells, facilitating activation of $CD4^+$ T cells and subsequent B cell-mediated antibody production. This process establishes a self-perpetuating cycle of antigen release and immune activation, contributing to chronic autoimmune progression (Weetman, 2021).

Overall, the structural and epitope information summarized from previous studies provides a useful framework for interpreting the experimental findings presented in this study. Although the precise structural origin of the isolated protein fraction remains unknown, the published structural information facilitates discussion of its observed immunoreactivity. Further peptide sequencing or high-resolution structural characterization will be required to determine the exact structural origin of the isolated protein fraction.

4. CONCLUSIONS

An approximately 50 kDa immunoreactive protein fraction was successfully isolated from the serum of hypothyroid patients with total protein concentrations ranging from 38.61 ± 0.60 to 65.13 ± 0.40 mg/mL and anti-TPO antibody levels ranging from approximately 20 to >600 IU/mL. The isolated fraction consistently appeared as a distinct ~50 kDa band by SDS-PAGE and exhibited characteristic protein functional groups by ATR-FTIR together with amino acid constituents identified by LC-MS/MS amino acid composition analysis, confirming its proteinaceous nature. Rabbit immunization induced a progressive humoral immune response, with anti-TPO IgG levels increasing from an OD_{405} of 0.152 before immunization to 0.555 at the eighth blood collection, while Western blot analysis demonstrated a specific immunoreactive ~50 kDa band only in the presence of immune rabbit serum. These findings

indicate that the isolated approximately ~50 kDa protein fraction possesses biochemical and immunogenic characteristics suitable for experimental polyclonal antibody production; however, further peptide-level protein identification and validation against native thyroid peroxidase are required to confirm its molecular identity and antibody specificity.

5. ACKNOWLEDGEMENT

The authors express their gratitude to the Directorate of Research and Community Engagement at Universitas Brawijaya for funding this research and its publication through the Pendanaan Penelitian Guru Besar 2024 (No. 02172. 7/UN10. F0901/B/KS/2024) and Pendanaan Penelitian Guru Besar 2025 (No. 06871. 3/UN10. F0901/B/PT/2025). Additional support for this research was provided by the Ministry of Finance of the Republic of Indonesia through RISPRO LPDP KEP-27/LPDP/2020 sub contract PRJ-26/LPDP/2020.

REFERENCES

Abramson, J. and G. Anderson (2017). Thymic Epithelial Cells. *Annual Review of Immunology*, **35**; 85–118

Akbar, R., H. Bashour, P. Rawat, P. A. Robert, E. Smorodina, T. S. Cotet, K. Flem-Karlsen, R. Frank, B. B. Mehta, M. H. Vu, T. Zengin, J. Gutierrez-Marcos, F. Lund-Johansen, J. T. Andersen, and V. Greiff (2022). Progress and Challenges for the Machine Learning-Based Design of Fit-for-Purpose Monoclonal Antibodies. *mAbs*, **14**(1); 2008790

Ali, R. A. H., N. A. Mahana, A. A. H. Mahdi, D. S. Wahb, A. Bakr, and A. M. Badr (2025). Anti-TPO and Anti-TSHR Antibodies in Combination with T3, T4, and TSH Exhibited a Diagnostic Curve for Hashimoto Patients. *The Journal of Basic and Applied Zoology*, **86**(1); 32

Anderson, N. L. and N. G. Anderson (2002). The Human Plasma Proteome: History, Character, and Diagnostic Prospects. *Molecular & Cellular Proteomics*, **1**(11); 845–867

Antonelli, A., S. M. Ferrari, A. Corrado, A. Di Domenicantonio, and P. Fallahi (2015). Autoimmune Thyroid Disorders. *Autoimmunity Reviews*, **14**(2); 174–180

Aulanni'am (2023). *Protein dan Analisisnya*. Inara Publisher, Malang, edisi revisi edition

Aulanni'am, A. B. Wijaya, D. K. Wuragil, A. P. W. Marhendra, A. D. Khairana, R. Rosandi, A. Rudijanto, and H. A. Tjahjono (2024). The Development of Monoclonal Antibody Against Thyroid-Stimulating Hormone for Congenital Hypothyroidism Screening in Indonesia. *Monoclonal Antibodies in Immunodiagnosis and Immunotherapy*, **43**(6); 153–159

Aulanni'am, D. K. Wuragil, D. W. Soeatmadji, Zulkarnain, and A. P. W. Marhendra (2018). Recombinant Protein Production from TPO Gen Cloning and Expression for Early Detection of Autoimmune Thyroid Diseases. *IOP Conference Series: Materials Science and Engineering*, **299**(1); 012013

Azzahra, F. D., L. N. Mulyani, T. Sabrina, and N. A. Fithri (2025). Liposome Photosensitizer with Enzyme from Black Soybean Tempeh: Formula Optimization and In Vitro Thrombolytic Activity Evaluation. *Science and Technology Indonesia*, **10**(3); 903–915

Benlaribi, R., Q. Gou, and H. Takaba (2022). Thymic Self-Antigen Expression for Immune Tolerance and Surveillance. *Inflammation and Regeneration*, **42**(1); 28

Benvenga, S. and R. Vita (2018). Thyroid Peroxidase. In I. Huhtaniemi and L. Martini, editors, *Encyclopedia of Endocrine Diseases*. Elsevier, 2 edition, pages 433–438

Bossowski, A., M. Moniuszko, M. Dabrowska, M. Rusak, M. Jeznach, A. Bodzenta-Łukaszyk, and A. Bossowska (2013). Role of Th17 Cells and IL-17, IL-23 Cytokines in Pathogenesis of Autoimmune Thyroid Disease in Children. *Thyroid Research*, **6**(Suppl 2); A8

Calsolaro, V., F. Niccolai, G. Pasqualetti, A. M. Calabrese, A. Polini, C. Okoye, S. Magno, N. Caraccio, and F. Monzani (2019). Overt and Subclinical Hypothyroidism in the Elderly: When to Treat? *Frontiers in Endocrinology*, **10**(MAR); 177

Carter, M. J., R. M. Mitchell, P. M. Meyer Sauteur, D. F. Kelly, and J. Trück (2017). The Antibody-Secreting Cell Response to Infection: Kinetics and Clinical Applications. *Frontiers in Immunology*, **8**; 630

Caturegli, P., A. De Remigis, and N. R. Rose (2014). Hashimoto Thyroiditis: Clinical and Diagnostic Criteria. *Autoimmunity Reviews*, **13**(4–5); 391–397

Crotty, S. (2019). T Follicular Helper Cell Biology: A Decade of Discovery and Diseases. *Immunity*, **50**(5); 1132–1148

Delahaut, P. (2017). Immunisation – Choice of Host, Adjuvants and Boosting Schedules with Emphasis on Polyclonal Antibody Production. *Methods*, **116**; 4–11

Espenbetova, M., N. Kuzmina, A. Zubkov, V. Akhmetova, Z. Zamanbekova, A. Krykpaeva, Z. Zhumanbayeva, K. Amrenova, Z. Smailova, and N. Glushkova (2022). Epitopes Specificity of Antibodies to Thyroid Peroxidase in Patients with Graves' Disease, Hashimoto's Thyroiditis and Overlap-Syndrome. *Journal of Clinical and Translational Endocrinology*, **27**; 100293

Ferrari, S. M., P. Fallahi, A. Antonelli, and S. Benvenga (2017). Environmental Issues in Thyroid Diseases. *Frontiers in Endocrinology*, **8**; 50

Ferrari, S. M., F. Ragusa, G. Elia, S. R. Paparo, V. Mazzi, E. Baldini, S. Benvenga, A. Antonelli, and P. Fallahi (2021). Precision medicine in autoimmune thyroiditis and hypothyroidism. *Frontiers in pharmacology*, **12**; 750380

Finkelstein, A. V. (2018). 50+ Years of Protein Folding. *Biochemistry (Moscow)*, **83**(Suppl. 1); S3–S18

Fiqriyana, M. A., Aulanni'am, and A. Roosdiana (2013). Characterization of Polyclonal Antibody Induced by Autoantibody TPO (Thyroidperoxidase) From Autoimmune Thyroid Disease (AITD) Serum with ELISA and Western Blotting. *Journal of Pure and Applied Chemistry Research*, **2**(1); 19–26

Gessulat, S., T. Schmidt, D. P. Zolg, P. Samaras, K. Schnatbaum, J. Zerweck, T. Knaute, J. Rechenberger, B. Delanghe,

A. Huhmer, U. Reimer, H. C. Ehrlich, S. Aiche, B. Kuster, and M. Wilhelm (2019). Prosit: Proteome-Wide Prediction of Peptide Tandem Mass Spectra by Deep Learning. *Nature Methods*, **16**(6); 509–518

Geyer, P. E., L. M. Holdt, D. Teupser, and M. Mann (2017). Revisiting Biomarker Discovery by Plasma Proteomics. *Molecular Systems Biology*, **13**(9); 942

Ghosh, R., J. E. Gilda, and A. V. Gomes (2014). The Necessity of and Strategies for Improving Confidence in the Accuracy of Western Blots. *Expert Review of Proteomics*, **11**(5); 549–560

Godlewska, M., K. D. Arczewska, M. Rudzińska, A. Łyczkowska, W. Krasuska, K. Hanusek, J. Ruf, M. Kiedrowski, and B. Czarnocka (2017). Thyroid Peroxidase (TPO) Expressed in Thyroid and Breast Tissues Shows Similar Antigenic Properties. *PLoS ONE*, **12**(6); e0179066

Godlewska, M., D. Gawel, A. M. Buckle, and J. P. Banga (2019). Thyroid Peroxidase Revisited—What's New? *Hormone and Metabolic Research*, **51**(12); 765–769

Greenfield, E. A. (2022). Immunizing Animals. *Cold Spring Harbor Protocols*, **2022**(7); 267–294

Gulla, S., M. C. Reddy, V. C. Reddy, S. Chitta, M. Bhanoori, and D. Lomada (2023). Role of Thymus in Health and Disease. *International Reviews of Immunology*, **42**(5); 347–363

Hammarlund, E., A. Thomas, I. J. Amanna, L. A. Holden, O. D. Slayden, B. Park, L. Gao, and M. K. Slifka (2017). Plasma Cell Survival in the Absence of B Cell Memory. *Nature Communications*, **8**(1); 1781

Hato, L., A. Vizcay, I. Eguren, J. L. Pérez-Gracia, J. Rodríguez, J. Gállego Pérez-Larraya, P. Sarobe, S. Inogés, A. L. Díaz de Cerio, and M. Santisteban (2024). Dendritic Cells in Cancer Immunology and Immunotherapy. *Cancers*, **16**(5); 981

Hempelmann, E. and K. Krafts (2017). The Mechanism of Silver Staining of Proteins Separated by SDS Polyacrylamide Gel Electrophoresis. *Biotechnic & Histochemistry*, **92**(2); 79–85

Hirahara, K. and T. Nakayama (2016). CD4+ T-Cell Subsets in Inflammatory Diseases: Beyond the Th1/Th2 Paradigm. *International Immunology*, **28**(4); 163–171

Hu, X., Y. Chen, Y. Shen, R. Tian, Y. Sheng, and H. Que (2022). Global Prevalence and Epidemiological Trends of Hashimoto's Thyroiditis in Adults: A Systematic Review and Meta-Analysis. *Frontiers in Public Health*, **10**; 1020707

Huang, L., X. Deng, R. Li, Y. Xia, G. Bai, K. H. M. Siddique, and P. Guo (2018). A Fast Silver Staining Protocol Enabling Simple and Efficient Detection of SSR Markers Using a Non-Denaturing Polyacrylamide Gel. *Journal of Visualized Experiments*, (134); 57192

Jankovic, J., M. Dettwiler, M. G. Fernández, E. Tièche, K. Hahn, S. April-Monn, M. S. Dettmer, M. Kessler, S. Rottenberg, and M. Campos (2021). Validation of Immunohistochemistry for Canine Proteins Involved in Thyroid Iodine Uptake and Their Expression in Canine Follicular Cell Thyroid Carcinomas (FTCs) and FTC-Derived Organoids. *Veterinary Pathology*, **58**(6); 1172–1180

Jin, Y., D. Shi, and L. Wang (2025). Application Value of Chemiluminescence Immunoassay in Thyroid Function Biochemical Testing. *Journal of Fluorescence*

Kaspar, H., K. Dettmer, W. Gronwald, and P. J. Oefner (2009). Advances in Amino Acid Analysis. *Analytical and Bioanalytical Chemistry*, **393**(2); 445–452

Khairana, A. D., S. Fiddaroini, A. B. Wijaya, R. Rosandi, A. Sabarudin, A. Safitri, W. Riawan, D. K. Wuragil, and Aulanniam (2025). Computational Analysis of TSHb Variants (Native, Mutated and Deleted) in Interaction with TSHR: Molecular Docking and Dynamic Simulations for Mechanistic Insights into Congenital Hypothyroidism. *Trends in Sciences*, **22**(8); 10086

Kirley, T. L. and A. B. Norman (2018). Unfolding of IgG Domains Detected by Non-Reducing SDS-PAGE. *Biochemical and Biophysical Research Communications*, **503**(2); 944–949

Klein, L., E. A. Robey, and C.-S. Hsieh (2019). Central CD4+ T Cell Tolerance: Deletion Versus Regulatory T Cell Differentiation. *Nature Reviews Immunology*, **19**(1); 7–18

Klubo-Gwiezdzinska, J. and L. Wartofsky (2022). Hashimoto Thyroiditis: An Evidence-Based Guide to Etiology, Diagnosis and Treatment. *Polish Archives of Internal Medicine*, **132**(3); 16222

Le, S. N., B. T. Porebski, J. McCoey, J. Fodor, B. Riley, M. Godlewska, M. Góra, B. Czarnocka, J. P. Banga, D. E. Hoke, I. Kass, and A. M. Buckle (2015). Modelling of Thyroid Peroxidase Reveals Insights into Its Enzyme Function and Autoantigenicity. *PLoS ONE*, **10**(12); e0142615

Lewis, S. M., A. Williams, and S. C. Eisenbarth (2019). Structure and Function of the Immune System in the Spleen. *Science Immunology*, **4**(33); eaau6085

Liu, T., Y. Wang, X. Luo, J. Li, S. A. Reed, H. Xiao, T. S. Young, and P. G. Schultz (2016). Enhancing Protein Stability with Extended Disulfide Bonds. *Proceedings of the National Academy of Sciences of the United States of America*, **113**(21); 5910–5915

Liu, Z., M. J. Tu, C. Zhang, J. L. Jilek, Q. Y. Zhang, and A.-M. Yu (2019). A Reliable LC-MS/MS Method for the Quantification of Natural Amino Acids in Mouse Plasma: Method Validation and Application to a Study on Amino Acid Dynamics During Hepatocellular Carcinoma Progression. *Journal of Chromatography B*, **1124**; 72–81

Loi Julia, S.-H. and L.-H. Gam (2020). SDS-PAGE Protein Profiling of a Few Commonly Consumed Beans. *Journal of Biotechnology and Bioengineering*, **4**(1)

Ma, S. G., Y. L. Qiu, H. Zhu, H. Liu, Q. Li, and C. M. Ji (2015). Novel Genetic Variants in the TPO Gene Cause Congenital Hypothyroidism. *Scandinavian Journal of Clinical and Laboratory Investigation*, **75**(8); 633–637

Makaraviciute, A., C. D. Jackson, P. A. Millner, and A. Ramanaviciene (2016). Considerations in Producing Preferentially Reduced Half-Antibody Fragments. *Journal of Immunological Methods*, **429**; 50–56

Mariam, S. H. S., R. Noorain, W. S. Tan, A. Arbakariya, and

O. A. Janna (2026). Purification and Characterization of Rabbit Polyclonal Immunoglobulin G Using DEAE Ion-Exchange Chromatography and Dynamic Light Scattering. *Protein Expression and Purification*, **242**; 106938

Marx, A., Y. Yamada, K. Simon-Keller, B. Schalke, N. Willcox, P. Ströbel, and C. A. Weis (2021). Thymus and Autoimmunity. *Seminars in Immunopathology*, **43**(1); 45–64

McLachlan, S. M. and B. Rapoport (2017). Thyroid Autoantibodies Display Both "Original Antigenic Sin" and Epitope Spreading. *Frontiers in Immunology*, **8**; 1845

McLeod, D. S. A. and D. S. Cooper (2012). The Incidence and Prevalence of Thyroid Autoimmunity. *Endocrine*, **42**(2); 252–265

Miller, J. F. A. P. (2020). The Function of the Thymus and Its Impact on Modern Medicine. *Science*, **369**(6503); eaba2429

Neto, V., S. Esteves-Ferreira, I. Inácio, M. Alves, R. Dantas, I. Almeida, J. Guimarães, T. Azevedo, and A. Nunes (2022). Metabolic Profile Characterization of Different Thyroid Nodules Using FTIR Spectroscopy: A Review. *Metabolites*, **12**(1); 53

Noor, Z., S. B. Ahn, M. S. Baker, S. Ranganathan, and A. Mohamedali (2021). Mass Spectrometry-Based Protein Identification in Proteomics: A Review. *Briefings in Bioinformatics*, **22**(2); 1620–1638

Nugroho, I. C., M. N. Amalia, M. R. Juniardi, E. B. Marhendra, N. A. Yanma, O. R. Adianingsih, S. Winarsih, N. Widodo, and V. Yurina (2026). Oral Immunization with Recombinant Lactococcus Lactis and Retinoic Acid Boost Immune Response in Mice. *Science and Technology Indonesia*, **11**(1); 55–64

Panjaitan, T. F. C., S. Fiddaroini, E. Suprayitno, Aulanni'am, and Hardoko (2025). Potential Analysis of Snakehead Fish Albumin Extract (Channa striata) as Immunostimulant and Anti-Inflammatory in Indomethacin-Induced Inflammatory Bowel Disease (IBD) Rats. *Science and Technology Indonesia*, **10**(3); 725–740

Patagar, P. M. and S. Rudrappa (2022). Autoimmune Thyroiditis in Adolescents: Two Different Presentations. *Karnataka Paediatric Journal*, **37**; 30–34

Pedersen, I. B. and P. Laurberg (2009). Antibodies to Thyroid Peroxidase and Thyroglobulin in Iodine Deficiencies. In *Comprehensive Handbook of Iodine: Nutritional, Biochemical, Pathological and Therapeutic Aspects*. Elsevier, pages 575–585

Pushpagiri, N., L. Gracelyn, and S. Nagalingam (2015). Prevalence of Subclinical and Overt Hypothyroidism in Infertile Women. *International Journal of Reproduction, Contraception, Obstetrics and Gynecology*, **4**(6); 1733–1738

Ragusa, F., P. Fallahi, G. Elia, D. Gonnella, S. R. Paparo, C. Giusti, L. P. Churilov, S. M. Ferrari, and A. Antonelli (2019). Hashimoto's Thyroiditis: Epidemiology, Pathogenesis, Clinic and Therapy. *Best Practice & Research: Clinical Endocrinology & Metabolism*, **33**(6); 101367

Ramadani, D., A. B. Wijaya, A. Srihardyastutie, D. K. Wuragil, R. Rosandi, A. Rudijanto, and Aulanni'am (2024). Characterization of TPO Enzyme and Its Immunogenicity in New Zealand White Rabbits (Oryctolagus cuniculus). *Jurnal Penelitian Pendidikan IPA*, **10**(12); 10645–10652

Raphael, I., R. R. Joern, and T. G. Forsthuber (2020). Memory CD4+ T Cells in Immunity and Autoimmune Diseases. *Cells*, **9**(3); 531

Raphael, I., S. Nalawade, T. N. Eagar, and T. G. Forsthuber (2015). T Cell Subsets and Their Signature Cytokines in Autoimmune and Inflammatory Diseases. *Cytokine*, **74**(1); 5–17

Rapoport, B. and S. M. McLachlan (2018). Reflections on Thyroid Autoimmunity: A Personal Overview from the Past into the Future. *Hormone and Metabolic Research*, **50**(12); 840–852

Rehlund, A. S. G., T. S. Canoy, D. S. Nielsen, M. N. Lund, and M. M. Poojary (2025). Protein Hydrolysis for Amino Acid Analysis Revisited. *Food Chemistry*, **495**; 146224

Rose, A., D. Funk, and R. Neiger (2016). Comparison of Refractometry and Biuret Assay for Measurement of Total Protein Concentration in Canine Abdominal and Pleural Fluid Specimens. *Journal of the American Veterinary Medical Association*, **248**(7); 789–794

Rothschild, K. J. (2016). The Early Development and Application of FTIR Difference Spectroscopy to Membrane Proteins: A Personal Perspective. *Biomedical Spectroscopy and Imaging*, **5**(3); 231–267

Ruterbusch, M., K. B. Pruner, L. Shehata, and M. Pepper (2020). In Vivo CD4+ T Cell Differentiation and Function: Revisiting the Th1/Th2 Paradigm. *Annual Review of Immunology*, **38**; 705–725

Salman, M. A., A. Rabiee, A. Salman, and T. E. Ftohy (2020). Antithyroid Peroxidase Antibodies and Histopathological Outcomes in Egyptian Patients Subjected to Total Thyroidectomy for Nonmalignant Nodular Goiter. *Research Square*

Shawkat Kawther, R., R. Tahir Lak, and S. Mohammed Zaki Abdullah (2022). The Role of Anti-TPO as an Additional Analytical Marker in Thyroid Disease Patients in Erbil City. *Diyala Journal of Medicine*, **23**(2); 120–130

Shehata, M., H. Saad Eldien, F. Meligy, and S. Bahaidarh (2019). The Possible Protective Role of Barley Seeds on the Spleen After Administration of Glucocorticoids in Adult Albino Rats: A Histological and Immunohistochemical Study. *Journal of Microscopy and Ultrastructure*, **7**(4); 171–180

Siriwardhane, T., K. Krishna, V. Ranganathan, V. Jayaraman, T. Wang, K. Bei, S. Ashman, K. Rajasekaran, J. J. Rajasekaran, and H. Krishnamurthy (2019). Significance of Anti-TPO as an Early Predictive Marker in Thyroid Disease. *Autoimmune Diseases*, **2019**; 1684074

Stebegg, M., S. D. Kumar, A. Silva-Cayetano, V. R. Fonseca, M. A. Linterman, and L. Graca (2018). Regulation of the Germinal Center Response. *Frontiers in Immunology*, **9**; 2469

Suan, D., C. Sundling, and R. Brink (2017). Plasma Cell and Memory B Cell Differentiation from the Germinal Center. *Current Opinion in Immunology*, **45**; 97–102

Takaba, H. and H. Takayanagi (2017). The Mechanisms of T

Cell Selection in the Thymus. *Trends in Immunology*, **38**(11); 805–816

Tater, A., A. Gupta, G. Upadhyay, A. Deshpande, R. Date, and I. Y. Tamboli (2021). In Vitro Assays for Characterization of Distinct Multiple Catalytic Activities of Thyroid Peroxidase Using LC-MS/MS. *Current Research in Toxicology*, **2**; 19–29

Tatulian, S. A. (2019). FTIR Analysis of Proteins and Protein–Membrane Interactions. In *Methods in Molecular Biology*, volume 2003. Humana Press, pages 281–325

Teijaro, J. R., D. Turner, Q. Pham, E. J. Wherry, L. Lefrançois, and D. L. Farber (2011). Cutting Edge: Tissue-Retentive Lung Memory CD4 T Cells Mediate Optimal Protection to Respiratory Virus Infection. *The Journal of Immunology*, **187**(11); 5510–5514

Tintor, K. Ninković, J. Milošević, and N. Polović (2024). Gaining Insight into Protein Structure via ATR-FTIR Spectroscopy. *Vibrational Spectroscopy*, **134**; 103726

Trifanescu, R. A. and C. Poiana (2019). Diagnosis and Management of Hypothyroidism in Adults. In *Advanced Practice in Endocrinology Nursing*. Springer International Publishing, pages 581–592

Tuska, H. S. A., A. M. Hariati, A. Sanusi, G. Ciptadi, B. Rumhayati, H. Susanto, G. Residiwati, and Aulanni'am (2025). Reproductive Toxicity and Histopathological Effects of Heavy Metal Exposure in Male Nile Tilapia from the Brantas River, Indonesia. *Biodiversitas*, **26**(10); 5169–5180

Uhlén, M., A. Bandrowski, S. Carr, A. Edwards, J. Ellenberg, E. Lundberg, D. L. Rimm, H. Rodriguez, T. Hiltke, M. Snyder, and T. Yamamoto (2016). A Proposal for Validation of Antibodies. *Nature Methods*, **13**(10); 823–827

Valentine, K. M., D. Davini, T. J. Lawrence, G. N. Mullins, M. Manansala, M. Al-Kuhlani, J. M. Pinney, J. K. Davis, A. E. Beaudin, S. S. Sindi, D. M. Gravano, and K. K. Hoyer (2018). CD8 Follicular T Cells Promote B Cell Antibody Class Switch in Autoimmune Disease. *The Journal of Immunology*, **201**(1); 31–40

Vancauwenberghe, T., A. Snoeckx, D. Vanbeckevoort, S. Dymarkowski, and F. M. Vanhoenacker (2015). Imaging of the Spleen: What the Clinician Needs to Know. *Singapore Medical Journal*, **56**(3); 133–144

Villela, L. F. d. A., L. C. C. d. Freitas, M. Brandão, L. Bachmann, and R. Iwakura (2018). Characterization of Thyroid Tissue Using Infrared Spectroscopy. *Archives of Head and Neck Surgery*, **47**(1); e0874

Wang, L., F.-S. Wang, and M. E. Gershwin (2015). Human Autoimmune Diseases: A Comprehensive Update. *Journal of Internal Medicine*, **278**(4); 369–395

Weetman, A. P. (2021). An Update on the Pathogenesis of Hashimoto's Thyroiditis. *Journal of Endocrinological Investigation*, **44**(5); 883–890

Weisel, F. and M. Shlomchik (2017). Memory B Cells of Mice and Humans. *Annual Review of Immunology*, **35**; 255–284

Williams, D. E., S. N. Le, D. E. Hoke, P. G. Chandler, M. Gora, M. Godlewska, J. P. Banga, and A. M. Buckle (2020). Structural Studies of Thyroid Peroxidase Show the Monomer Interacting with Autoantibodies in Thyroid Autoimmune Disease. *Endocrinology*, **161**(2); bqaa016

Yadav, V., D. Dabar, A. D. Goel, M. Bairwa, A. Sood, P. Prasad, S. S. Agarwal, and S. Nandeshwar (2021). Prevalence of Hypothyroidism in Pregnant Women in India: A Meta-Analysis of Observational Studies. *Journal of Thyroid Research*, **2021**; 5515831

Yamano, T., J. Nedjic, M. Hinterberger, M. Steinert, S. Koser, S. Pinto, N. Gerdes, E. Lutgens, N. Ishimaru, M. Busslinger, B. Brors, B. Kyewski, and L. Klein (2015). Thymic B Cells Are Licensed to Present Self Antigens for Central T Cell Tolerance Induction. *Immunity*, **42**(6); 1048–1061

Zhang, C.-H., X.-J. Liu, Y.-F. Wang, J.-H. Lu, H.-Y. Zheng, S. Xiong, M.-Y. Zhang, and Q.-Y. Liu (2007). Immune Responses and Histopathological Changes in Rabbits Immunized with Inactivated SARS Coronavirus. *Virologica Sinica*, **22**(5); 425–431

Zhu, J. (2018). T Helper Cell Differentiation, Heterogeneity, and Plasticity. *Cold Spring Harbor Perspectives in Biology*, **10**(10); a030338

Zhu, J., H. Yamane, and W. E. Paul (2010). Differentiation of Effector CD4+ T Cell Populations. *Annual Review of Immunology*, **28**; 445–489